Chem Soc Rev

REVIEW ARTICLE

View Article Online
View Journal

Check for updates

Cite this: DOI: 10.1039/d5cs00195a

Recent advances in catalytic asymmetric metalloid–hydrogen bond insertion of transition-metal carbenes

Shuyue Zhang and Ming-Hua Xu *

Over recent decades, transition-metal-catalyzed asymmetric carbene insertion into metalloid–hydrogen bonds (B–H/Si–H/Ge–H) has become a prominent research area. This review summarizes recent enantioselective strategies for constructing chiral organoboron, organosilicon, and organogermanium compounds through carbon–metalloid bond formation. Approaches are classified by chirality induction modes, with emphasis on transition-metal catalysts paired with precisely designed chiral ligands, including bisoxazolines, dienes, carboxylates, and diimines. Mechanistic correlations between ligand architectures and stereocontrol are discussed. Additionally, environmentally friendly biocatalytic approaches using engineered enzymes are also highlighted.

Received 5th April 2025

DOI: 10.1039/d5cs00195a

rsc.li/chem-soc-rev

Published on 09 June 2025. Downloaded by Shaanxi Normal University on 6/10/2025 4:15:58 AM.

1. Introduction

Metalloids, which exhibit properties of both metals and non-metals, have garnered significant attention from synthetic chemists due to their unique chemical characteristics, such as variable hybridization and electronic tunability. Their corresponding metalloid–hydrogen bonds (*e.g.*, B–H, Si–H, and Ge–H) serve as essential scaffolds for catalytic transformations, enabling the incorporation of metalloid-functionalized groups into organic frameworks. These transformations have demonstrated broad applications in pharmaceuticals, agrochemicals, and materials science.[1]

Transition-metal catalysts, particularly organometallic catalysts, have revolutionized modern synthetic organic chemistry

Shenzhen Grubbs Institute and Department of Chemistry, Guangdong Provincial Key Laboratory of Catalysis, Southern University of Science and Technology, Xueyuan Rd., Shenzhen 518055, China. E-mail: xumh@sustech.edu.cn

Shuyue Zhang

Shuyue Zhang was born in Hunan in 1991. He obtained his MSc in Chemistry with Medicinal Chemistry (2015, supervisor: Prof. Alan Spivey) at Imperial College London. Then he received his PhD in 2020 under the supervision of Prof. Andrew Smith at the University of St Andrews. After working in Sygnature Discovery, Nottingham, for two years on drug discovery (2020–2022), he joined the Xu Group at Southern University of Science and Technology as a postdoctoral researcher in 2022, focusing on the synthesis of stereogenic boron compounds involving transition metal catalysis.

Ming-Hua Xu

Ming-Hua Xu is currently a professor in the Department of Chemistry at Southern University of Science and Technology (SUSTech) and Shenzhen Grubbs Institute. He obtained his PhD at Shanghai Institute of Organic Chemistry (SIOC), Chinese Academy of Sciences in 1999. Following postdoctoral research at the University of Virginia and Georgetown University Medical Center, he joined the faculty at SIOC as an associate professor in 2003. He was appointed as a full professor at Shanghai Institute of Materia Medica, Chinese Academy of Sciences in 2005. He joined SUSTech in 2018. His research interest mainly related to asymmetric synthesis and chiral drugs, including development of new chiral ligands/catalysts; new synthetic methods and strategies, synthesis of bioactive compounds, and small molecule drug discovery.

Published on 09 June 2025. Downloaded by Shaanxi Normal University on 6/10/2025 4:15:58 AM.

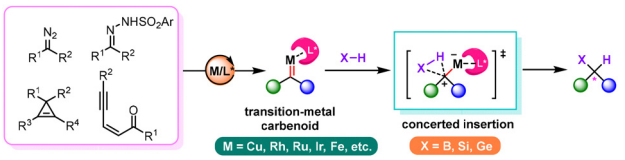

Scheme 1 Catalytic asymmetric metalloid–hydrogen insertion reactions.

by providing efficient and selective pathways to construct diverse molecular architectures.[2] A cornerstone of this field is the formation of transition metal carbenes, typically generated from diazo compounds and related derivatives. These carbenes are highly reactive intermediates, and by carefully tuning the electronic and steric properties of the catalytic system, highly selective bond-forming transformations, such as metalloid–hydrogen (X–H) insertions (where X represents boron, silicon, or germanium), can be achieved in a concerted manner (Scheme 1). Over the past two decades, this catalytic asymmetric X–H insertion strategy has been extensively studied to construct chiral organometalloid compounds with high enantioselectivity and diastereoselectivity. For example, B–H insertions have provided access to chiral boron-containing compounds, which are valuable synthetic intermediates.[3,4] Similarly, Si–H insertion reactions yield silicon-stereogenic silanes, which are important in both materials science and pharmaceutical industries.[5] More recently, the emerging field of Ge–H insertion chemistry has shown promise for constructing novel organogermanium frameworks. In addition to the metal-catalyzed approach, photochemical strategy has started to appear, even if it is limited in scope and lacks enantioselectivity. For example, visible-light-induced, metal- and photocatalyst-free B–H insertion reactions have been developed recently, enabling the formation of C–B bonds under mild conditions.[6,7]

In recent years, a number of review articles have been published by research groups worldwide, addressing this strategy from various perspectives including carbene precursors, transition metal catalysts, and biocatalysis.[5,8–13] Several reviews have also touched upon the application of this strategy in synthesizing less-explored boron-stereogenic compounds.[14–17] However, a comprehensive yet concise review that covers all three types of metalloid–hydrogen (B–H, Si–H, Ge–H) bond insertions, with a particular emphasis on the role of diverse chiral ligand systems, remains lacking. The design of chiral ligands and metal catalysts to create a sterically and electronically defined environment is critical for controlling the reaction pathway and stereochemical outcomes. This review aims to provide a comprehensive overview of recent progress and advancements in catalytic asymmetric X–H insertion, highlighting the origins of chiral induction and their synthetic utility.

2. Ligand controlled catalytic asymmetric B–H insertion

Constructing optically active organoboron compounds through asymmetric B–H insertion has emerged as a pivotal strategy in organic synthesis and pharmaceutical industry. The success of these transformations hinges on the use of chiral ligands to control the stereochemical outcome of the B–H insertion step.

Since the groundbreaking copper/chiral bisoxazoline (BOX)-catalyzed protocol developed by Zhou and Zhu in 2013, this field has garnered significant attention from synthetic chemists. Subsequent advancements, including the introduction of novel ligands such as chiral dienes (Xu, 2015)[18] and chiral dirhodium carboxylates (Zhou and Zhu, 2017),[19] have further expanded the scope of this methodology. This chapter provides an overview of recent progress, emphasizing the diverse and versatile nature of ligands employed in asymmetric B–H insertion reactions.

2.1. Chiral bisoxazoline (BOX) ligands

Modern synthetic community has witnessed the development and application of chiral bisoxazoline ligand in the synthesis of optically pure molecules, due to the ease of its synthesis and ability to fine-tune steric and electronic properties to achieve optimal stereochemical control.[20] In 2013, Zhou and Zhu developed the first copper-catalyzed asymmetric B–H bond insertion using a spiro-cyclic BOX ligand (Scheme 2),[21] a significant advancement that coincided with the Rh-catalyzed B–H insertion strategy of diazocarbonyl compounds reported by Curran and co-workers.[22] These two studies, published nearly simultaneously, marked a pivotal moment in the field of B–H insertion. By employing $Cu(MeCN)_4PF_6$ as the catalyst, $NaBAr^F$ as the additive, and the chiral spiro-BOX ligand, they obtained a broad range of enantiopure phosphine-borane adducts with high enantiomeric excess (91–94% ee) and yield (86–96%). These adducts were further transformed into valuable organoboron building blocks, such as β-hydroxy pinacolborane. Later, the same group expanded the scope of this transformation by using α-aryl diazoketones as carbene precursors under the same catalytic system.[23] However, only moderate enantioselectivity

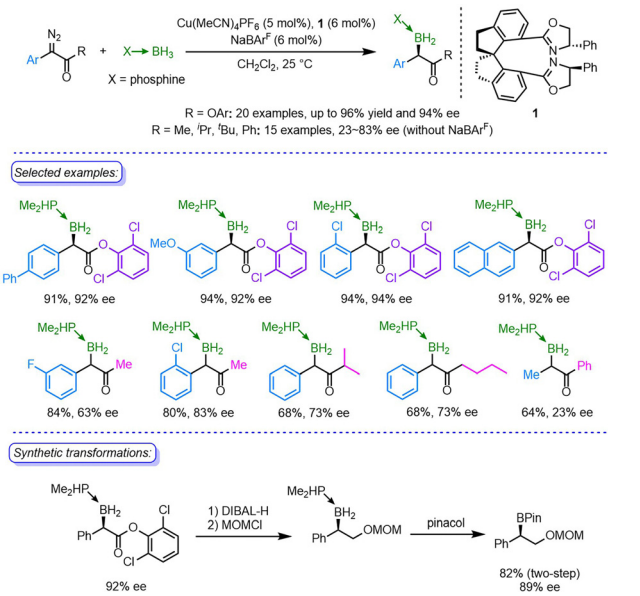

Scheme 2 Cu(I)/chiral spiro-BOX catalyzed B–H insertion with α-aryl diazocarbonyl compounds.

This journal is © The Royal Society of Chemistry 2025

Published on 09 June 2025. Downloaded by Shaanxi Normal University on 6/10/2025 4:15:58 AM.

(23–83% ee) was achieved with the spiro-BOX ligand, and α-methyl diazoketone proved incompatible, yielding only 23% ee and 64% yield.

Further advancements were made by Gouverneur and co-workers, who demonstrated a copper-catalyzed asymmetric B–H insertion between PPh_3-borane and aryl trifluorodiazoalkane (Scheme 3a).[24] Both spiro-BOX and C_2-symmetric indene-derived BOX ligands were effective under the Cu(I)/NaBAr^F catalytic system, affording products with 72% ee and 81% ee, respectively, in moderate yields. An important breakthrough came in early 2024, when Song and co-workers successfully employed α-aryl diazophosphonates as carbene precursors in a highly enantioselective B–H insertion, achieving up to 97% yield and 98% ee using a similar Cu(I)/indene-BOX ligand system (Scheme 3b).[25] Mechanistic studies revealed a concerted B–H insertion pathway for the copper carbene intermediate. The transition state in favor of the *S*-enantiomer minimized steric hindrance between the ligand and the substrate by forming favorable π–π stacking between aromatic groups, underscoring the critical role of ligand design in attaining high stereoselectivity.

In addition to traditional aryldiazoacetates as donor–acceptor carbene precursors, vinyldiazoacetates have also been employed in generating metal carbenoids for catalytic X–H insertion processes,[26,27] providing access to valuable allyl-functionalized building blocks. However, challenges remain in handling these substrates to prevent undesired decomposition, such as pyrazole formation. In 2020, Vilotijevic and co-workers reported the synthesis of allylborane–phosphine adducts using a Cu(I)/BOX catalytic system.[28] Unfortunately, efforts to achieve an asymmetric variant of this reaction using enantiomerically enriched BOX ligands were unsuccessful. In the sole instance reported, only a low enantiomeric excess (30% ee) and a moderate yield (64%) were obtained. This result suggests that significant optimization of the system is still required to enable efficient and highly enantioselective catalysis (Scheme 4).

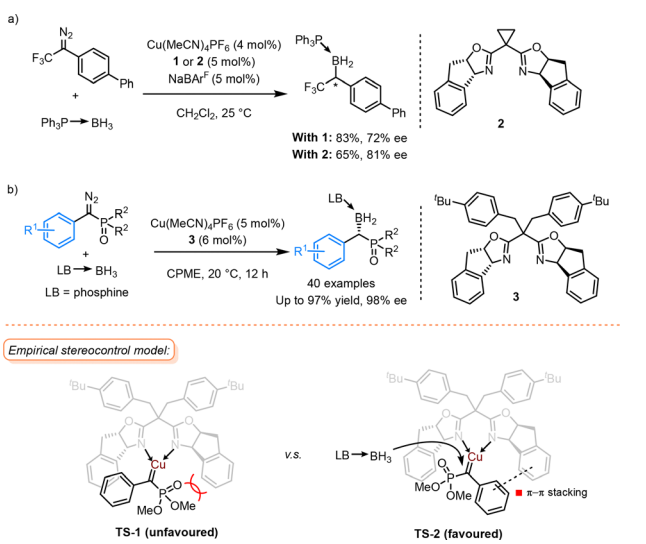

Scheme 3 Cu(I)/chiral BOX catalyzed B–H insertion with (a) α-aryl diazoalkane and (b) diazophosphonates.

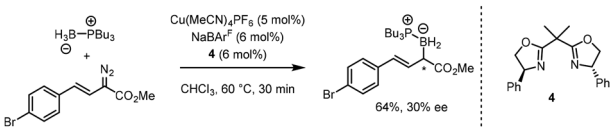

Scheme 4 Cu(I)/chiral BOX catalyzed B–H insertion with vinyldiazoacetate.

Building upon their earlier work of using highly strained cyclopropenes as carbene precursors in catalytic B–H insertion,[29] Zhu and co-workers developed an elegant strategy for highly regio-, stereo-, and enantioselective B–H insertion with metal α-silylcarbenoids derived from 1-silylcyclopropenes, providing access to chiral γ,γ-disubstituted allylic *gem*-silylboranes.[30] By employing Cu(MeCN)$_4$PF$_6$ as the catalyst in combination with a chiral BOX ligand, a broad range of 3,3-disubstituted 1-silylcyclopropenes and amine/pyridine boranes were found to be compatible in the reaction, giving exclusively *E*-configured products with excellent enantioselectivities (Scheme 5). Since the

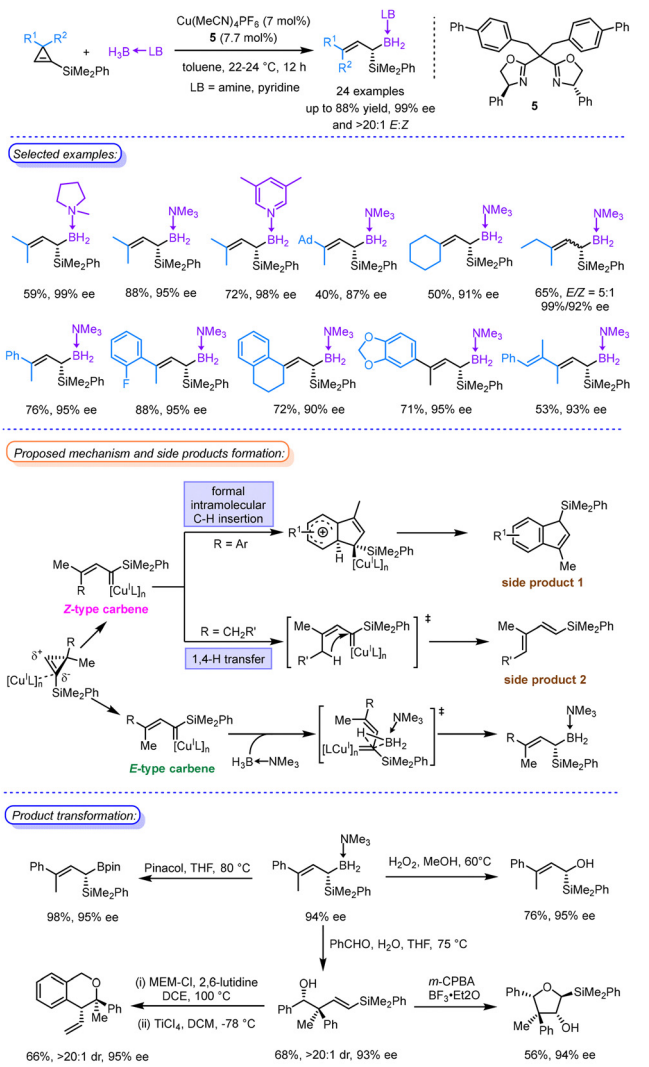

Scheme 5 Cu(I)/chiral BOX catalyzed B–H insertion with 1-silylcyclopropenes.

Published on 09 June 2025. Downloaded by Shaanxi Normal University on 6/10/2025 4:15:58 AM.

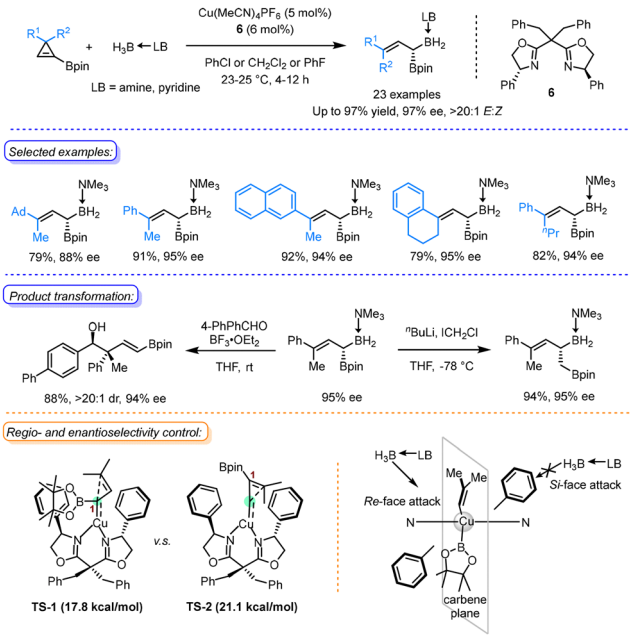

Scheme 6 Cu(I)/chiral BOX catalyzed B–H insertion with 1-borylcyclopropenes.

electron density of cyclopropene at C1 is higher than that at C2, the regioselectivity was achieved by the attack of electrophilic Cu catalyst at C1 to cleave the C1–C3 bond. For unsymmetrical cyclopropenes with aryl/alkyl substituents, minor byproducts were observed, resulting from either 1,4-hydride transfer or formal intramolecular C–H insertion of the *Z*-type carbene intermediate. Importantly, the enantiomeric excess was preserved during the derivatization of the insertion products into α-silyl alcohols, pinacol boronates, and other functionalized derivatives.

Subsequently, the same group extended this approach to the enantioselective B–H insertion of α-boryl carbenes derived from 1-borylcyclopropenes, utilizing a similar Cu(I)/BOX catalytic system.[31] This method enabled the synthesis of a series of highly enantioenriched *gem*-diborons with up to 97% ee (Scheme 6). These *gem*-diborons were further transformed through various synthetic processes, including BPin homologation, allylboration, Suzuki coupling, and oxidation, without any loss of enantiopurity. Computational studies revealed that the polarization of the cyclopropene's π-bond by the conjugated empty 2p orbital of the boryl group directed the selective electrophilic attack of the copper center at C1 of the cyclopropene. This was further supported by the lower Gibbs energy of the C1-cleavage transition state compared to alternative pathways. By adopting a conformation where the BPin group is perpendicular to the carbene plane, the α-boryl carbene minimized its conjugation and stabilized itself through σ-donation. This conformation, combined with the face shielding provided by the chiral BOX ligand, ensured that the nucleophilic attack of the borane occurred selectively onto the *Re* face of the carbene, achieving high enantioselectivity.

Shifting focus from the construction of carbon-stereogenic centers *via* B–H insertion, Song and Yu made significant contributions to the synthesis of boron-stereogenic compounds through a copper-catalyzed enantioselective and diastereoselective desymmetric B–H insertion using 2-arylpyridine boranes and diazo compounds.[32] Symmetric bis-aryl diazo compounds reacted smoothly with 2-arylpyridine boranes to yield enantioenriched boron-stereogenic products with excellent enantioselectivity. In contrast, unsymmetric α-aryl diazoacetates enabled the formation of products featuring two consecutive stereogenic centers with high stereocontrol (Scheme 7). The synthetic utility of this approach was further demonstrated through additional B–H insertions, reductions, and cross-coupling reactions. The bulky ester group, positioned away from steric interactions, facilitated π–π stacking between the phenyl rings of the ligand and substrate, ensuring that the insertion predominantly occurred on the less hindered carbene face, thereby achieving

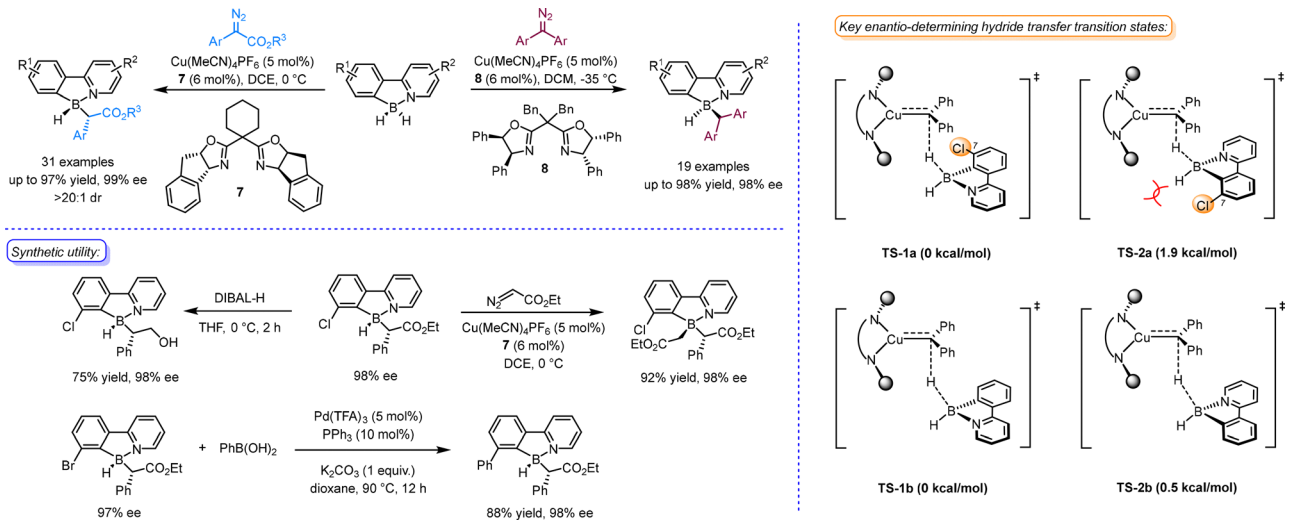

Scheme 7 Cu(I)/chiral BOX catalyzed B–H insertion with 2-arylpyridine boranes.

 This journal is © The Royal Society of Chemistry 2025

Published on 09 June 2025. Downloaded by Shaanxi Normal University on 6/10/2025 4:15:58 AM.

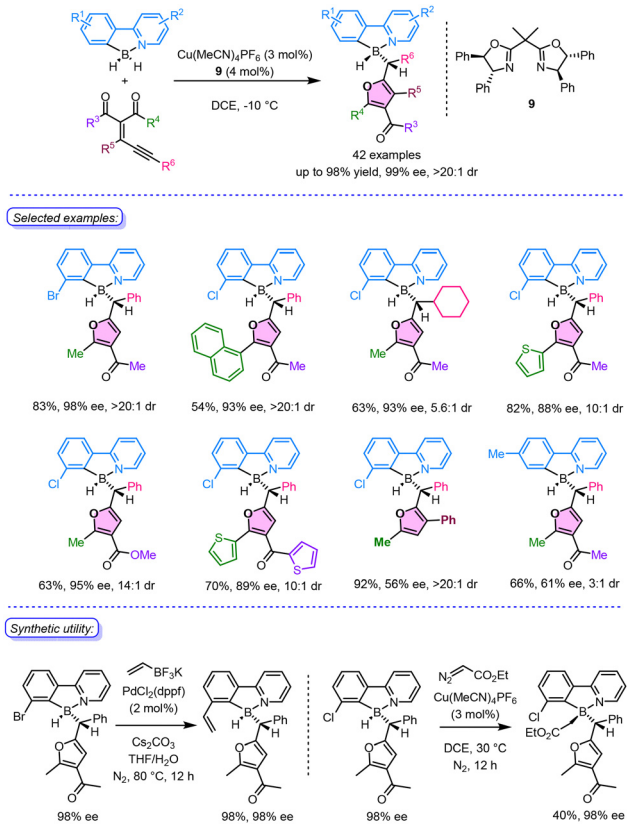

Scheme 8 Cu(I)/chiral BOX catalyzed B–H insertion with ene–yne–ketones.

high enantioselectivity. DFT calculations of the key transition states revealed that substituents at the C7-position of the 2-arylpyridine borane significantly enhanced stereocontrol by introducing steric interactions to differentiate between the two B–H bonds during desymmetrization.

In a subsequent study, Song and co-workers replaced the diazoester carbene precursors with less toxic and operationally simpler ene–yne–ketones, achieving a highly efficient Cu(I)-catalyzed B–H bond insertion with 2-arylpyridine boranes.[33] This method provided access to functionalized furans bearing adjacent boron and carbon stereogenic centers with high diastereo- and enantioselectivity (Scheme 8). Notably, a decrease in both diastereo- and enantioselectivity was observed for 2-arylpyridine borane substrates lacking substituents at either the C4 or C7 positions. The insertion products were successfully transformed *via* Suzuki coupling and second B–H insertion without loss of enantiopurity. Additionally, Grignard addition and aldol-type condensation enabled the synthesis of tertiary alcohols and α,β-unsaturated carbonyl compounds.

2.2. Chiral diene ligands

Chiral diene ligands have emerged as a powerful tool for constructing chiral molecules, demonstrating remarkable efficiency and selectivity in a wide range of enantioselective transformations.[34] Their ability to form stable coordination complexes with transition metals, such as rhodium, iridium, underpins many highly enantioselective processes, including reactions involving diazo compounds. The rigid, well-defined frameworks of chiral dienes impose specific spatial arrangements in the transition state of the catalytic cycle, enabling the synthesis of enantioenriched molecules.

The application of chiral diene ligands in asymmetric B–H insertion was first realized in early 2015 when our group reported the pioneering rhodium(I)-catalyzed asymmetric carbene insertion into B–H bonds using α-diazo carbonyl compounds and amine-borane adducts (Scheme 9),[18] providing access to highly enantioenriched organoborons. A broad range of α-diazoesters and α-diazoketones were compatible, yielding B–H insertion products with diverse aryl or alkyl substituents. The synthetic utility of this approach was further demonstrated by transforming the insertion products into valuable intermediates, such as β-hydroxy pinacol borate esters and β-boryl alcohols, without loss of stereoselectivity. A concerted transition state was proposed, involving simultaneous interaction between the Rh(I)-carbene species and the B–H bond. In the empirical stereochemical model, the diene ligand oriented the carbene moiety orthogonal to the coordination plane, positioning the bulky ester group away from steric interactions and forming a π–π stacking between benzene rings of the substrate and the diene ligand. Therefore, the B–H insertion takes place predominantly from the less hindered carbene face at the site adjacent to Cl to provide products with high level of enantioselectivity.

Thereafter, Perekalin and co-workers also conducted research in this field in 2021 by designing a novel tetrafluorobenzobarrelene-derived chiral diene ligand (TFB). The Rh(I)/TFB complex demonstrated high enantioselectivity and reactivity in

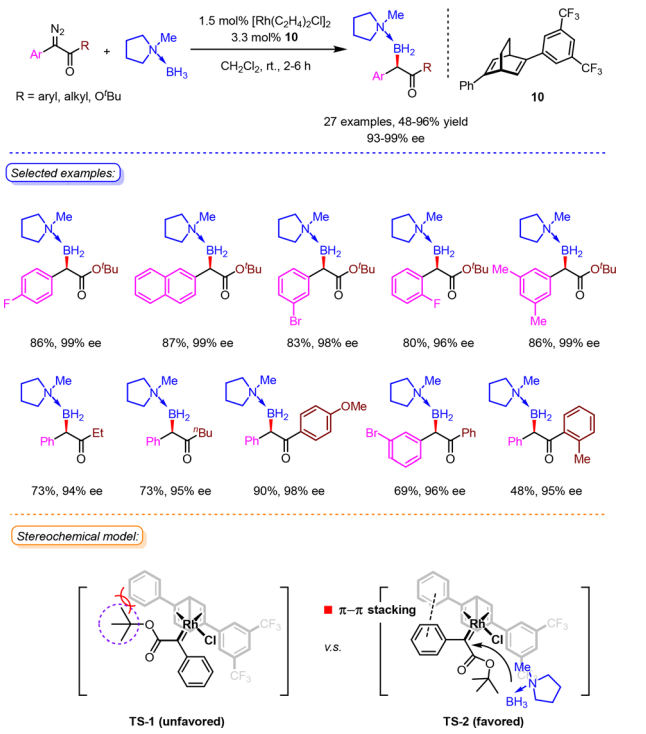

Scheme 9 Rh(I)/chiral diene catalyzed asymmetric B–H insertion.

Published on 09 June 2025. Downloaded by Shaanxi Normal University on 6/10/2025 4:15:58 AM.

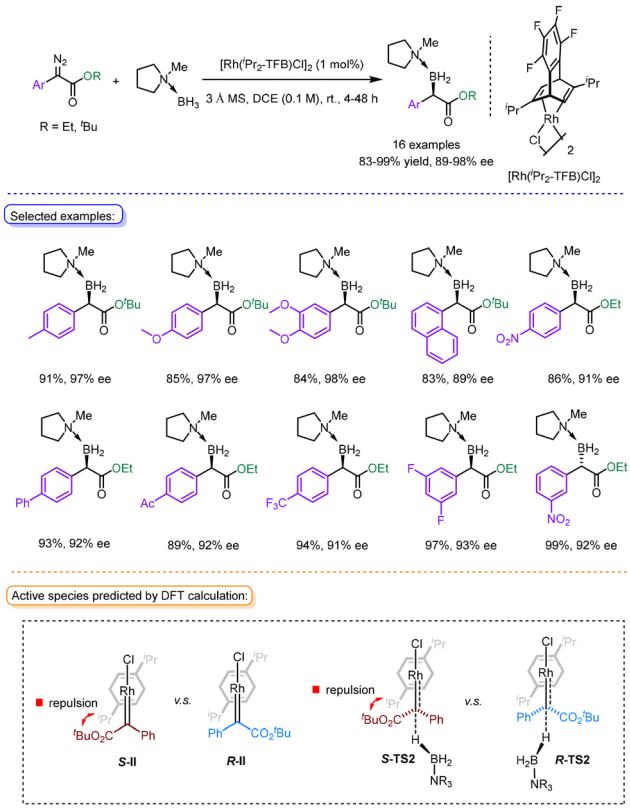

Scheme 10 Rh(I)/TFB catalyzed asymmetric B–H insertion.

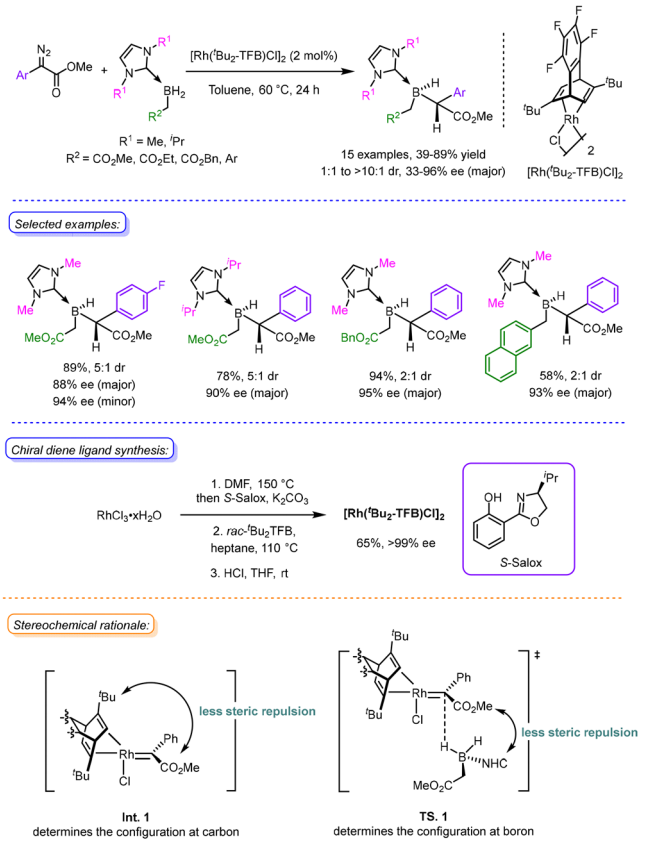

Scheme 11 Rh(I)/TFB catalyzed B–H insertion to access chiral boron compounds.

the asymmetric insertion of diazo compounds into B–H bonds, accommodating a variety of aryl diazo esters, including those with electron-donating, electron-withdrawing, and sterically hindered substituents (Scheme 10).[35] DFT calculations predicted the formation of two possible carbene intermediates, *R*-II and *S*-II, with the activation barrier for *R*-II formation being 1.8 kcal mol^{-1} lower than that for *S*-II. This energy difference correlated with the observed enantioselectivity, favoring the *R*-product with >90% ee. The steric repulsion between the ester group on the carbene intermediate and the ^{i}Pr substituent on the chiral diene ligand ensured that borane addition to the carbene complex could only occur from one specific orientation, resulting in high enantiomeric purity of the organoboron product.

In 2024, the same group expanded the application of the Rh(I)/TFB catalytic system by achieving the synthesis of stereogenic boranes through the asymmetric insertion of diazo compounds into the B–H bond of prochiral NHC-BH_2R (Scheme 11).[36] A TFB-derived chiral diene ligand featuring two bulky ^{t}Bu substituents was synthesized with high optical purity (>99% ee) *via* coordination with an auxiliary chiral *S*-Salox ligand. The B–H insertion demonstrated broad compatibility with various aryldiazoacetates, delivering high yields (up to 94%) and enantioselectivities (up to 96% ee), albeit with moderate diastereoselectivities (1:1 to 10:1). Notably, sterically hindered boranes and pyridine boranes exhibited poor reactivity under these conditions. The stereochemical outcome at the boron center was governed by steric repulsion between the CO_2Me group and the NHC moiety, while the configuration at the carbon center was determined by minimizing steric clashes between the ^{t}Bu group on the ligand and the CO_2Me group.

Almost simultaneously, our group reported the use of diaryldiazomethanes as carbene precursors in a highly enantioselective cationic Rh(I)/diene-catalyzed B–H insertion (Scheme 12).[37] A wide range of diaryldiazomethanes, including those with electron-donating and electron-withdrawing substituents, were evaluated. Notably, higher enantioselectivity was observed when the carbene bore electronically dissimilar aryl groups, a trend supported by Hammett analysis correlating enantioselectivity with electronic differences. The newly designed chiral diene ligand, featuring *ortho*-amidophenyl substituents, introduced restricted rotation around the arene ring and conformational locking. This structural feature enforced the boron hydride to approach the carbene exclusively through the *Re*-face. Depending on the electronic properties of the two arene rings on the diaryldiazomethanes, only one optimal π–π stacking interaction was possible, directing the reaction towards a single enantiomer.

More recently, our group extended the generality of this Rh(I)/chiral diene-catalyzed asymmetric B–H insertion strategy to more challenging α-alkyl diazoacetates.[38] To address competing side reactions such as β-hydride migration and intramolecular C–H insertion, the Rh(I)/diene catalytic system was employed and compared with other transition metal catalysts, including copper(I)/(II), rhodium(II)/(III), ruthenium(II), and iridium(I). Under optimal conditions, the Rh(I)/chiral diene system exclusively

 This journal is © The Royal Society of Chemistry 2025

Published on 09 June 2025. Downloaded by Shaanxi Normal University on 6/10/2025 4:15:58 AM.

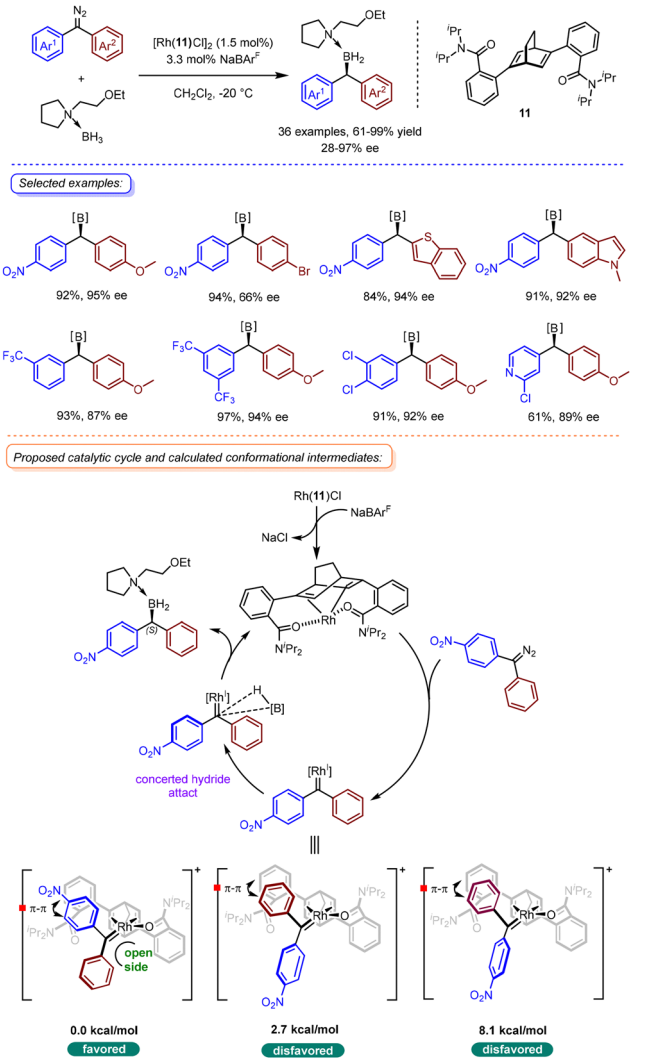

Scheme 12 Cationic Rh(I)/chiral diene catalyzed B–H insertion with diaryldiazomethanes.

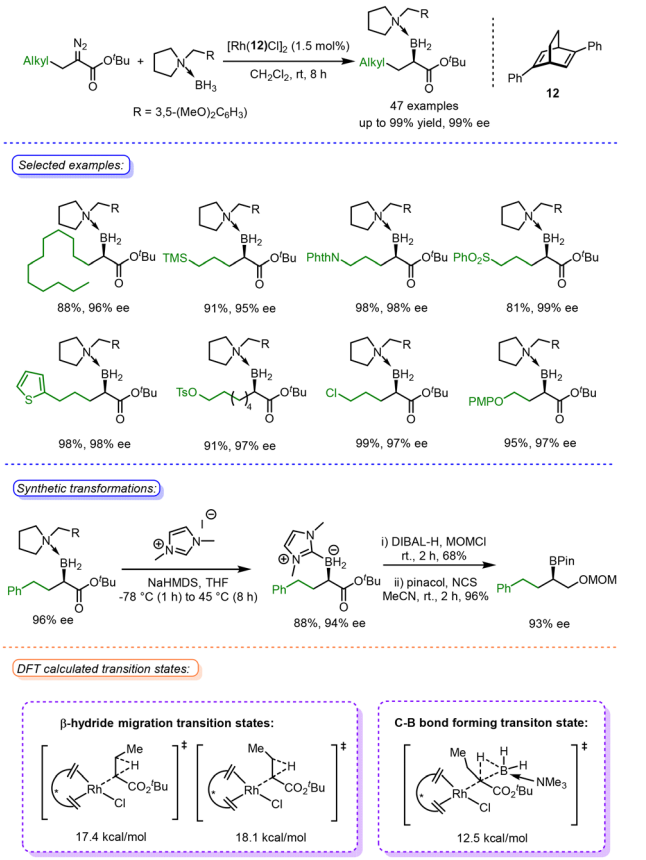

Scheme 13 Cationic Rh(I)/chiral diene catalyzed B–H insertion with α-alkyl diazoacetates.

afforded highly enantioenriched alkylboranes (Scheme 13). A variety of straight-chain, branched, and functionalized α-alkyl diazoacetates, including heterocyclic scaffolds, were compatible with the reaction conditions. Mechanistically, DFT calculations revealed that the β-hydride migration pathway has a significantly higher activation barrier (17.4 kcal mol^{-1} or 18.1 kcal mol^{-1}) compared to the carbene insertion pathway (12.5 kcal mol^{-1}). This computational finding is consistent with the experimentally observed preference for the carbene insertion route. In addition, the approach of the borane was sterically hindered on one side by the ligand framework, allowing insertion to occur exclusively at the less hindered face of the carbene. The resulting chiral alkylboranes were further transformed into valuable building blocks, such as boronic esters, amino alcohols, and diols, demonstrating the synthetic utility of this methodology.

2.3. Chiral carboxylate ligands

The design and application of chiral dirhodium(II) complexes as catalysts for asymmetric metal carbenoid reactions have attracted considerable interest over the past few decades.[39] The dinuclear scaffolds are well-suited to support chiral ligands, such as carboxylates, carboxamidates, and phosphonates, creating a well-defined chiral environment for enantioselective transformations (Fig. 1).[40] In 2017, Zhu and Zhou pioneered the use of dirhodium complexes with chiral carboxylate ligands in asymmetric B–H insertion, employing ene–yne–ketones as carbene precursors (Scheme 14).[19] Unlike copper catalysts with chiral ligands, which exhibited poor stereochemical control in such transformations, the dirhodium system successfully delivered trisubstituted furans in up to 96% ee. This method was compatible with a variety of substituted ene–yne–ketones, including those with ester and sulfonyl groups. The synthetic utility of the insertion products was demonstrated through condensation with pinacol and *N*-methyl imidodiacetic acid (MIDA), as well as oxidation to secondary alcohols, all without loss of enantioselectivity.

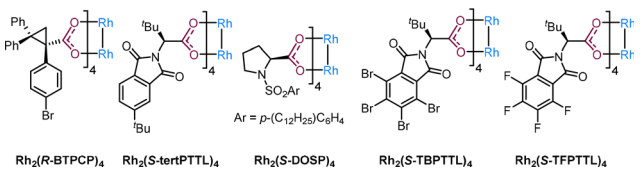

Fig. 1 Chiral dirhodium(II) complexes discussed in this chapter.

Published on 09 June 2025. Downloaded by Shaanxi Normal University on 6/10/2025 4:15:58 AM.

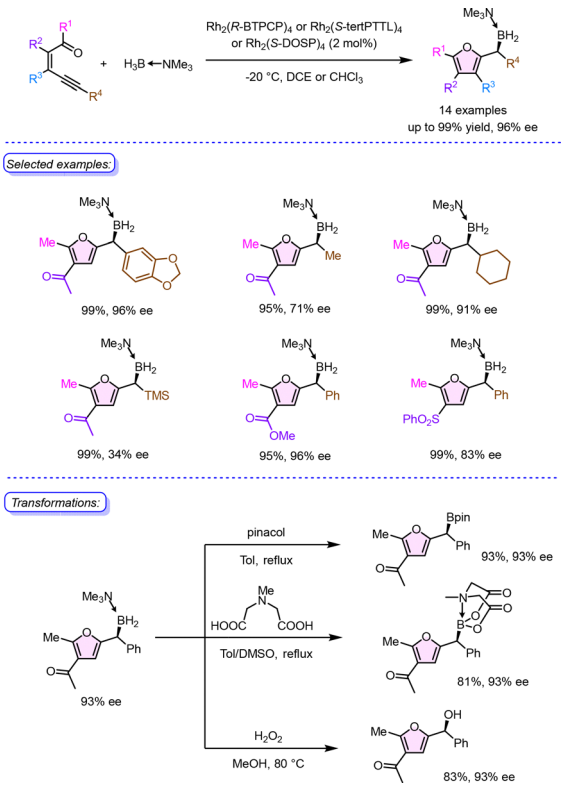

Scheme 14 Rh(II)/chiral carboxylates catalyzed B–H insertion with ene–yne–carbonyls.

Shortly thereafter, the same group achieved highly enantioselective B–H insertion by generating diazo compounds *in situ* from tosylhydrazones, using a similar dirhodium chiral carboxylate catalytic system.[41] This approach circumvented the limitations of traditional diazo compounds, which often require electron-withdrawing groups for stability, thereby enhancing synthetic flexibility. Both amine and pyridine boranes were tested, and two distinct catalytic systems were developed to optimize enantioselectivity for different substrates: Rh_2(*R*-BTPCP)$_4$ for pyridine-borane adducts with aryl–alkyl ketones and Rh_2(*S*-TBPTTL)$_4$ for Me_3N-borane adducts with acetophenone derivatives (Scheme 15). The practicality of this strategy was demonstrated through gram-scale synthesis and the derivatization of products into valuable synthetic building blocks.

Using the same dirhodium chiral carboxylate catalytic system Rh_2(*S*-TBPTTL)$_4$, Zhu and co-workers also achieved the asymmetric synthesis of *gem*-diarylmethine boranes in 2021, significantly expanding the scope for chiral C–B bond formation.[42] This transformation demonstrated broad substrate compatibility, accommodating a wide range of *gem*-diaryl diazomethanes, including those with electron-withdrawing and electron-donating aryl rings, heterocycles, and even *ortho*-substituted aryl rings (Scheme 16). Hammett analysis revealed a positive linear correlation between enantioselectivity and the electronic differences between the two aryl substituents. DFT calculations further elucidated that the enantioselectivity originates from steric differences in the transition states, where the electron-rich aryl ring

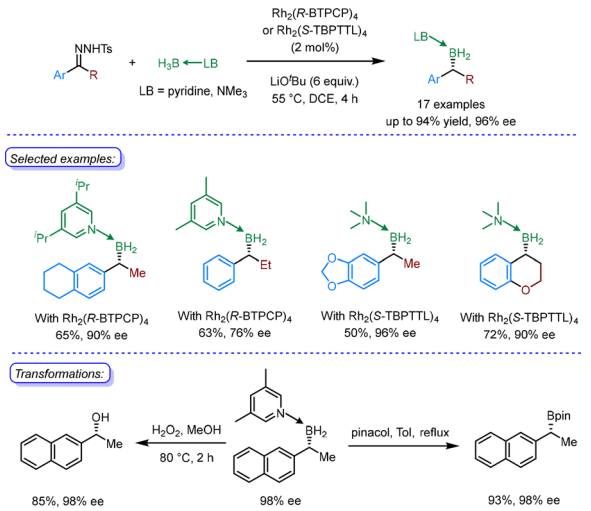

Scheme 15 Rh(II)/chiral carboxylates catalyzed B–H insertion.

aligns co-planarly with the carbene p-orbital, while the electron-deficient ring tilts out of the plane, creating an asymmetric environment around the catalyst.

The scope of dirhodium/chiral carboxylate-catalyzed B–H insertion was further expanded by the same group to enable the highly enantioselective synthesis of chiral propargylic boron compounds using aryl propargylic sulfonylhydrazones as carbene precursors.[43] This transformation exhibited a broad substrate scope, achieving yields of up to 99% and enantioselectivities of up to 97% ee under mild reaction conditions (Scheme 17). Chiral propargylic boron compounds, traditionally obtained from optically active starting materials, can now be efficiently accessed as valuable intermediates through this protocol. Furthermore, synthetic derivatization of these compounds successfully furnished enantioenriched molecules such as allenyl borates, propargyl alcohols, homopropargylic alcohols, and aryltriazole boranes, highlighting the versatility of this method.

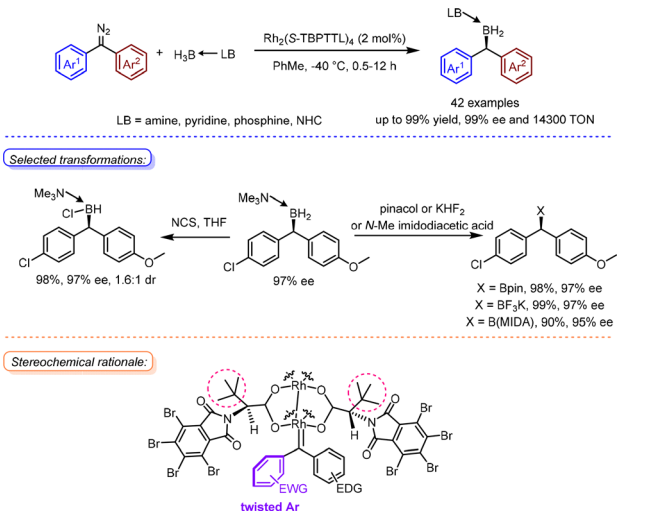

Scheme 16 Rh(II)/chiral carboxylates catalyzed B–H insertion with *gem*-diaryl diazomethanes.

 This journal is © The Royal Society of Chemistry 2025

Published on 09 June 2025. Downloaded by Shaanxi Normal University on 6/10/2025 4:15:58 AM.

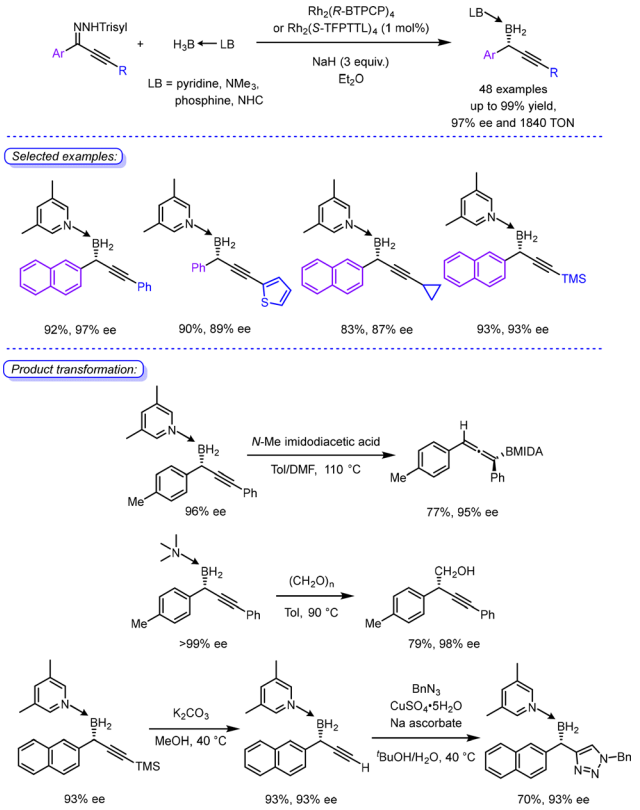

Scheme 17 Rh(II)/chiral carboxylates catalyzed B–H insertion with *gem*-diaryl diazomethanes.

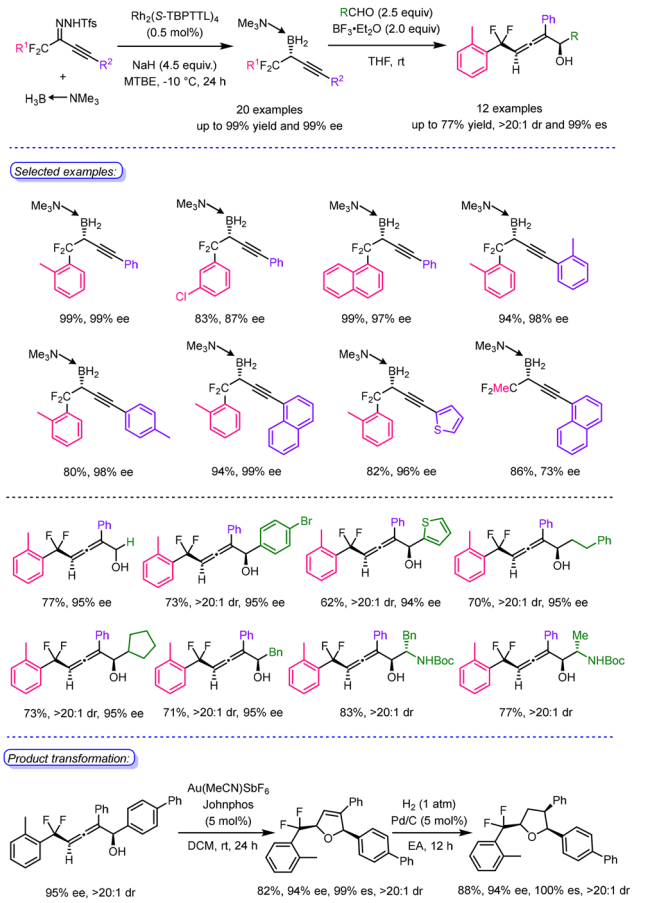

Scheme 18 Rh(II)/chiral carboxylates catalyzed B–H insertion to build chiral *gem*-difluoroalkyl fragments.

Chiral *gem*-difluoroalkyl fragments (R–CF_2–C) are prevalent in bioactive molecules, offering enhanced stability and biological activity due to their unique physicochemical properties. Leveraging a similar B–H insertion strategy, Zhu and co-workers developed an efficient and highly enantioselective synthesis of *gem*-difluoroalkyl propargylic boranes using *gem*-difluoroalkyl alkynyl *N*-triftosylhydrazones as substrates.[44] Treatment of the obtained propargylic boranes with aldehydes under Lewis acidic conditions enabled the synthesis of *gem*-difluoroalkyl α-allenols bearing both axial and central chirality with excellent regioselectivity and retention of enantiomeric purity (Scheme 18). Additionally, these α-allenols were further converted into *gem*-difluoroalkyl dihydrofuran or tetrahydrofuran derivatives, demonstrating the synthetic versatility and potential of this approach for accessing complex chiral molecules.

2.4. Other ligands and enzymatic catalysis

The highly enantioselective catalytic B–H insertion reaction could also be achieved using a Ru(II)–Pheox complex, as demonstrated in the seminal work by Iwasa (2021).[45] This catalyst, synthesized from readily available amino alcohol and benzyl chloride precursors, exhibited remarkable efficiency in catalyzing reactions between Lewis base-borane adducts and sterically hindered diazoesters. The insertion products were obtained in up to 94% yield with exceptional enantioselectivity (up to 98% ee) (Scheme 19). Mechanistic studies revealed that during the formation of the Ru–carbene intermediate, the bulky ester group of the diazo substrate is oriented away from the phenyl ring of the ligand to minimize steric repulsion. In the key concerted B–H insertion transition state, the phosphine or amine-borane adduct preferentially approaches the carbene from the less hindered *Re*-face, leading to the formation of the corresponding enantioenriched product.

In addition to traditional transition metal-catalyzed boron-capturing protocols, the development of genetically programmed platforms for the biosynthesis of chiral organoboranes using engineered enzymes has emerged as a transformative approach in this field. Arnold and co-workers pioneered this direction by demonstrating that specific mutations in wild-type cytochrome *c* enzyme (*Rma* cyt *c*) enabled highly enantioselective B–H insertion with diazoesters and NHC-boranes, achieving remarkable enantioselectivity of up to >99% ee and a total turnover number (TTN) of 3090 (Scheme 20a).[46] Through targeted mutational tuning, both enantiomers of the products became accessible. Building upon this groundbreaking work, Arnold and Houk extended the enzymatic platform to the synthesis of versatile α-trifluoromethylated organoborons using a broad range of trifluorodiazo alkanes, achieving up to 2870 TTN and 97% ee (Scheme 20b).[47] Structural analysis revealed that key mutations in the active-site residues (V75S, M99A, M100L, M103D, and Y44I) of the heme protein *Rma* cyt *c* were crucial for optimizing the enzyme's activity and selectivity.

Published on 09 June 2025. Downloaded by Shaanxi Normal University on 6/10/2025 4:15:58 AM.

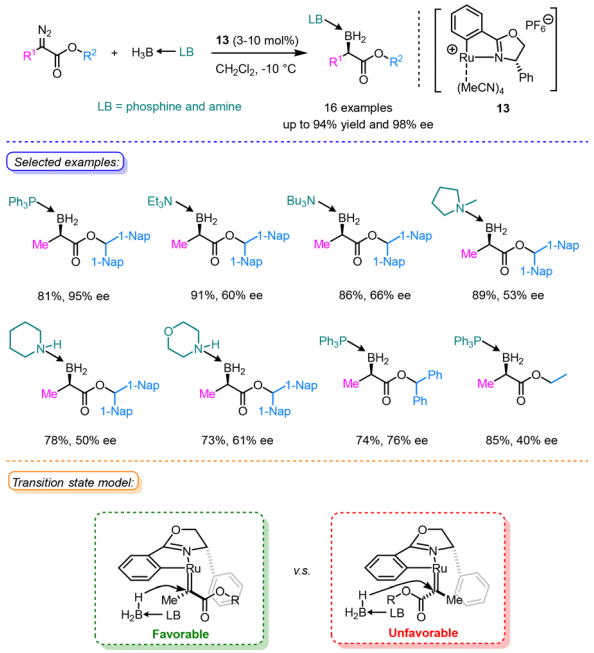

Scheme 19 Ru(II)/Pheox catalyzed B–H insertion.

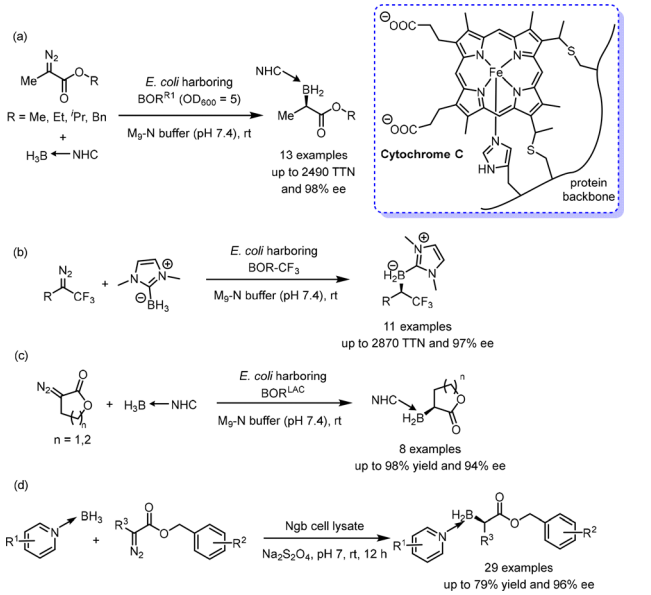

Scheme 20 (a)–(d) Biocatalytic asymmetric B–H insertions with heme protein and different carbene precursors.

The scope of biocatalytic carbene insertion was further expanded to cyclic lactone-based carbenes by the same research group.[48] This advancement demonstrated high selectivity and efficiency for the insertion of 5- and 6-membered lactone carbenes, with up to 24 500 total turnovers and 94% ee. However, the 7-membered lactone carbene exhibited significantly reduced catalytic activity and enantioselectivity, which was attributed to its highly twisted conformation (Scheme 20c). More recently, Lin and co-workers explored the engineering of human neuroglobin (Ngb), another heme protein, to develop an alternative biocatalytic platform for carbene transfer.[49] This system effectively catalyzed reactions with pyridine- and quinoline-boranes, as well as a wide range of α-methyl diazoesters, achieving up to 79% yield and 96% ee (Scheme 20d). Nevertheless, the system showed limitations with sterically demanding substrates, such as cyclopropane-substituted diazoesters, which resulted in reduced yields and enantioselectivities.

3. Ligand controlled catalytic asymmetric Si–H insertion

Catalytic asymmetric Si–H bond insertion has been recognized as a powerful synthetic strategy for constructing silicon–carbon bonds with high enantioselectivity. Silicon-containing molecules, owing to their versatile applications, serve as key intermediates in organic synthesis, functional materials in electronics and photonics, and valuable scaffolds in drug discovery.[50] Their unique chemical properties, including tunable hydrophobicity, thermal stability, and electronic modulation, render them indispensable in advanced material science and medicinal chemistry.[51] This chapter, presented in chronological order, provides an overview of recent progress in the application of various ligand types, such as chiral dirhodium complexes, chiral diimines, chiral bisoxazoline (BOX), and chiral dienes in effectively controlling the enantioselectivity of these reactions.

3.1. Chiral carboxylate/phosphonate ligands

The pioneering application of chiral dirhodium(II) complexes in asymmetric Si–H bond insertion with diazoesters and silanes was dated back to 1996, when Doyle and Moody reported their seminal work using chiral dirhodium(II) carboxylates or carboxamidates, achieving modest enantioselectivities ranging from 7% to 47% ee.[52] Subsequently, Davies and co-workers made significant advancements by developing highly enantioselective Si–H insertion reactions of vinylcarbenoids, yielding a series of enantioenriched allylsilanes.[53] These reactions were conducted at a stringent temperature of −78 °C, with NMR-calculated ee values ranging from 77% to 95% (Scheme 21). However, the allylsilane products exhibited instability during chromatography purification or fractional distillation, which limited their broader synthetic utility.

In 2006, Corey introduced an alternative strategy for the catalytic enantioselective synthesis of 6-silylated 2-cyclohexenones *via* Rh(II)/chiral carboxylate-catalyzed Si–H insertion of α-diazo-α,β-enones.[54] This transformation was found sensitive to the steric properties of the silanes employed. While triethylsilane and *tert*-butyldimethylsilane were well-tolerated, other silanes, such as triphenylsilane, resulted in lower yields

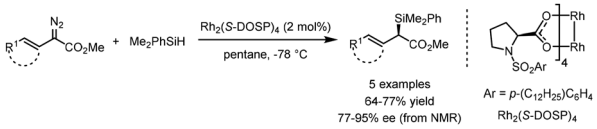

Scheme 21 Rh(II)/chiral carboxylates catalyzed B–H insertion with vinyldiazoacetates.

This journal is © The Royal Society of Chemistry 2025

Published on 09 June 2025. Downloaded by Shaanxi Normal University on 6/10/2025 4:15:58 AM.

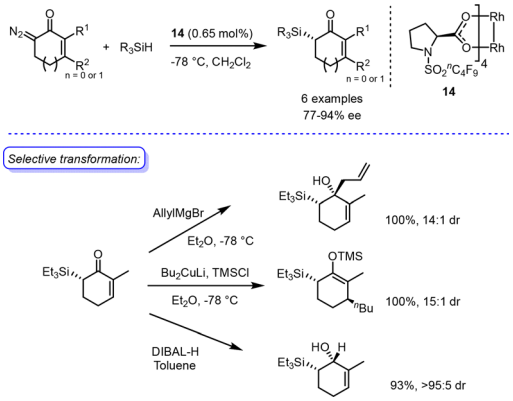

Scheme 22 Rh(II)/chiral carboxylates catalyzed B–H insertion with α-diazo-α,β-enones.

and enantioselectivities (Scheme 22). The enantioenriched silylated cyclohexenones were further explored in Lewis acid-catalyzed Diels–Alder reactions with cyclopentadiene. However, the strong electron-donating effect of the silyl group led to low conversion and regioselectivity. Conversely, the silyl group proved to be a valuable stabilizing and stereodirecting element in subsequent diastereoselective conjugate additions and reductions.

Building on their previous work on catalytic asymmetric B–H insertion using ene–yne–ketones as carbene precursors (Scheme 14), Zhu and co-workers discovered that chiral dirhodium tetracarboxylate complexes could also effectively catalyze enantioselective Si–H insertion with similar carbene precursors.[55] Under mild reaction conditions, excellent yields and enantioselectivities were achieved when less bulky silanes or silanes with electron-rich silicon centers were employed. The reaction demonstrated broad substrate tolerance, accommodating various aryl-, alkyl-, and cycloalkenyl-terminated carbonyl–ene–ynes (Scheme 23). Kinetic studies identified the Si–H bond insertion step as rate-determining. A stereoselective induction model was proposed to explain the high enantioselectivity, wherein the specific conformation of the ligands and the orientation of the furyl/phenyl group relative to the carbene plane directed the silane to approach the carbene center from the less-hindered *Si*-face, resulting in the formation of the *S*-configuration at the carbon stereocenter.

In 2020, Shaw and Franz achieved a significant breakthrough in the construction of silicon-stereogenic centers—a relatively underexplored area compared to carbon-based stereocenters---by developing the first enantioselective synthesis of silicon-stereogenic silanes *via* Rh(II)-chiral carboxylate-catalyzed Si–H insertion of donor/donor diarylcarbenes.[56] The scope of the reaction was evaluated using various prochiral silanes, including methylarylsilanes and bulky silanes, which afforded high yields and varying degrees of enantioselectivity. Notably, *ortho*-substituted phenyl groups in the prochiral diazo substrates improved stereoselectivity and yield by minimizing off-cycle azine formation (Scheme 24). In the chiral environment of the dirhodium catalyst, the stereoselectivity was further induced by a twisting effect caused by *ortho*-substitution on the phenyl ring, which directed the silane to attack the carbene selectively from

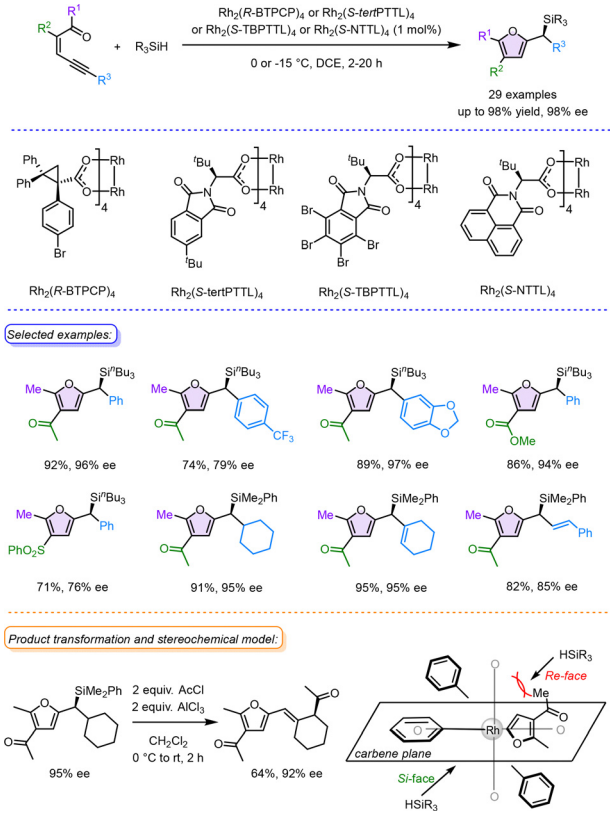

Scheme 23 Rh(II)/chiral carboxylates catalyzed B–H insertion with alkynes.

the less hindered face. Further synthetic transformations, such as the conversion to silanols, dehydrocoupling products, and intramolecular C–H silylation products, highlighted the synthetic utility of these silicon-stereogenic silanes.

In parallel, Zhou, Zhu, and Houk developed a novel class of D_4-symmetric chiral dirhodium catalysts featuring spirophosphate ligands. These catalysts demonstrated the ability to differentiate the prochiral faces of diarylcarbenes based on the electronic properties of substituents, enabling highly efficient enantioselective Si–H insertion reactions (Scheme 25).[57] Unlike the sterically controlled approach of Shaw and Franz, mechanistic studies revealed that electron-rich aryl rings adopted a coplanar orientation with the carbene plane, while electron-deficient rings remained orthogonal in the favored diastereomeric transition state. This electronic preference was confirmed by a linear relationship between the difference in transition-state energies and the Hammett constants of the substituents. The rigid D_4-symmetric dirhodium catalyst reinforced this electronic bias by fixing the carbene orientation, enabling precise enantiocontrol by directing the silane to approach one face of the carbene preferentially.

Expanding on their successful application of alkynyl carbenes—generated *in situ* from alkynyl sulfonylhydrazones for the synthesis of chiral propargylboranes (Schemes 17 and 18), Zhu and co-workers further established a well-designed enantioselective Si–H insertion strategy catalyzed by chiral spirophosphate dirhodium(II) complexes (Scheme 26).[58] Under

Published on 09 June 2025. Downloaded by Shaanxi Normal University on 6/10/2025 4:15:58 AM.

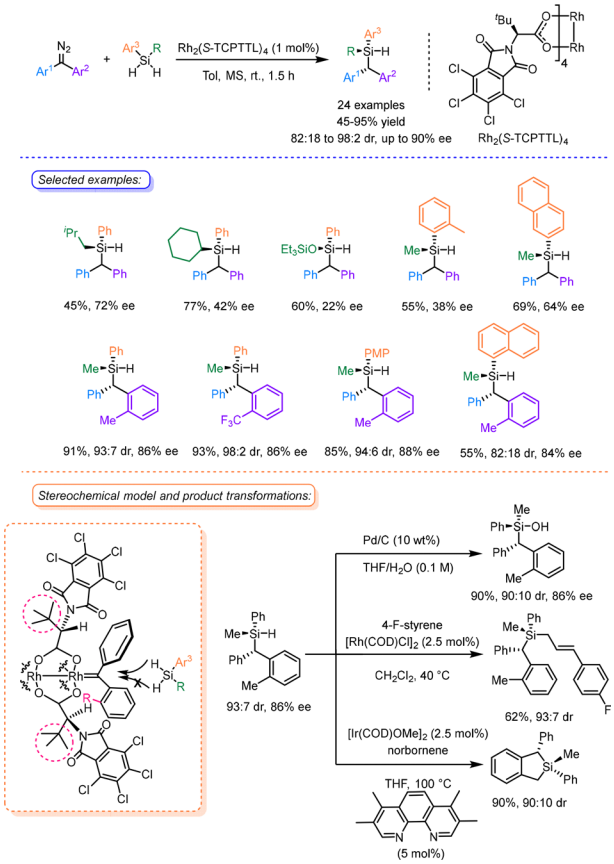

Scheme 24 Rh(II)/chiral carboxylates catalyzed B–H insertion to construct Si-stereogenic silanes.

optimized conditions, both aryl and aliphatic-substituted alkynyl hydrazones reacted with a wide range of silanes to afford products in high yields and promising enantioselectivities. Density functional theory (DFT) calculations indicated that the enantioselectivity arose from the sterically crowded pocket created by the chiral spiro-phosphate ligand, which forced the silane to approach the *Re*-face of the carbene intermediate. Additionally, the isolated propargylsilanes underwent stereospecific isomerization to chiral allenylsilanes in the presence of a catalytic amount of $(Ph_3P)_2PtO_2$, achieving high enantiospecificity through a point-to-axial chirality transfer.

3.2. Chiral Schiff base/salen ligands

Transition metal catalysts featuring chiral Schiff base ligands with diimine scaffolds have found extensive synthetic applications, primarily due to their ease of synthesis and structural tunability, which facilitate reaction optimization.[59] The first application of these ligands in enantioselective Si–H bond insertion reactions, using α-diazophenylacetates as carbene precursors, was reported by Zhou and co-workers in 2008. They employed a $Cu(OTf)_2$ catalyst combined with a newly designed chiral spiro-diimine ligand based on a spirobiindane backbone, achieving a series of chiral silanes with excellent enantioselectivities (90–99% ee) and high yields (Scheme 27a).[60] Subsequently, Panek expanded the scope of this transformation by

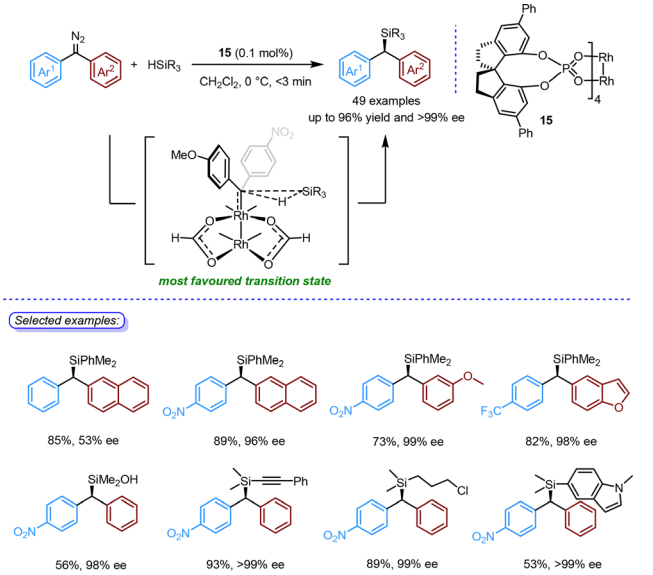

Scheme 25 Rh(II)/chiral spiro phosphate catalyzed B–H insertion of diarylcarbenes.

utilizing α-diazovinylacetates, previously explored by Davies,[53] as carbene precursors for the synthesis of chiral crotylsilanes. This approach yielded moderate enantioselectivities (70–78% ee), and

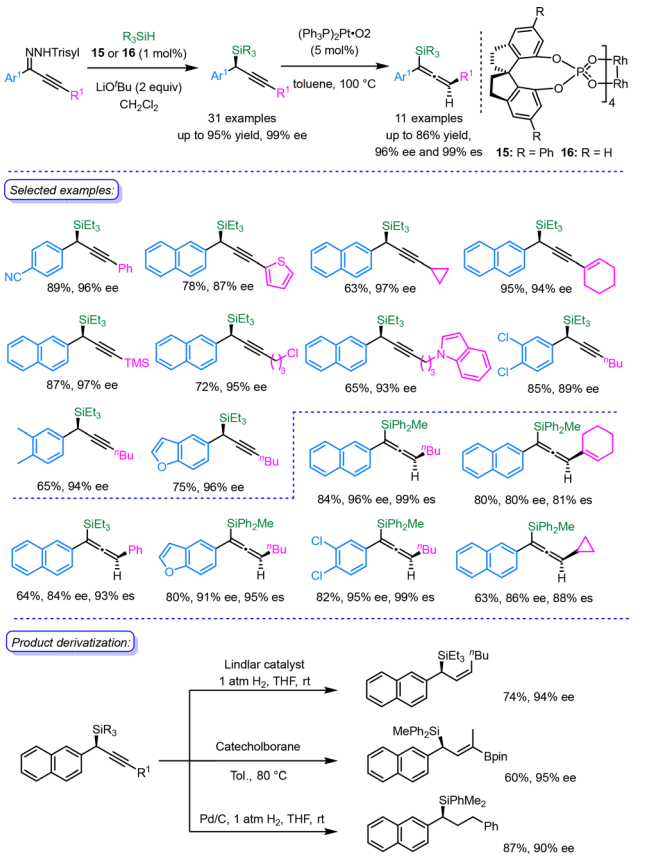

Scheme 26 Rh(II)/chiral spiro phosphate catalyzed B–H insertion of alkynyl sulfonylhydrazones.

This journal is © The Royal Society of Chemistry 2025

Published on 09 June 2025. Downloaded by Shaanxi Normal University on 6/10/2025 4:15:58 AM.

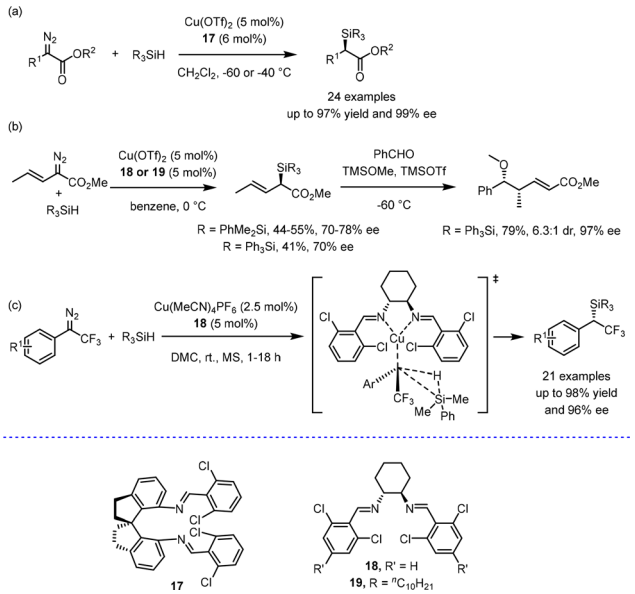

Scheme 27 (a)–(c) Application of chiral diimine ligands in asymmetric Si–H bond insertion with different carbene precursors.

the resulting enantioenriched silanes were effectively applied in vinylogous aldol reactions (Scheme 27b). For comparison, Panek also demonstrated that employing a chiral dirhodium carboxylate complex could improve the enantioselectivity to as high as 97% ee.[61] More recently, Gandon and Ollevier reported the synthesis of (1-aryl-2,2,2-trifluoroethyl)silanes with excellent yields and enantioselectivities using 1-aryl-2,2,2-trifluoro-1-diazoethanes as carbene precursors.[62] This reaction utilized a Cu(I)/chiral diimine catalytic system in the environmentally friendly solvent dimethyl carbonate (Scheme 27c). Mechanistic studies revealed that the stereoselectivity originated from a HOMO/LUMO-controlled attack of the Si–H bond on the carbene center, with the early transition state dictating the observed stereoisomer.

In addition to copper-based catalytic systems with chiral diimine ligands, iridium(III)-salen complexes have also been employed in enantioselective Si–H insertion reactions. Katsuki and co-workers demonstrated the efficacy of Ir(III)-salen complexes in highly efficient catalytic Si–H insertions with both α-aryldiazoesters and the more challenging α-alkyldiazoesters, showcasing their ability to suppress the competitive β-hydride elimination pathway.[63] The use of prochiral silanes was also explored, affording products containing both stereogenic silicon and carbon centers with diastereomeric ratios up to 50 : 1 and enantioselectivities up to 99% ee (Scheme 28). The concave shape of the salen ligand played a crucial role in enhancing enantioselectivity and suppressing β-hydride elimination by providing precise control over the carbenoid conformation.

Building on these advancements, Che and co-workers investigated the use of *cis*-β-ruthenium(II) complexes with sterically bulky salen ligands as catalysts for enantioselective carbene insertion into Si–H bonds.[64] Under light irradiation (300 W incandescent lamp), decarbonylation of the Ru(II) complex took place to generate the active catalytic species, which efficiently

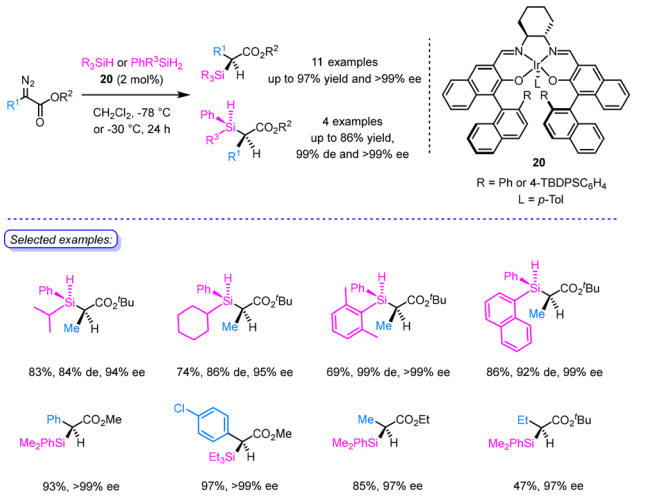

Scheme 28 Ir(III)/salen catalyzed enantioselective Si–H insertion with diazoesters.

reacted with diazo compounds and silanes to yield silyl esters with moderate to good enantioselectivities of up to 84% ee (Scheme 29). The key *cis*-β-[Ru(salen)(CO)(CAr$_2$)] carbene complex was detected using high-resolution ESI-MS and isolated for X-ray structural analysis, revealing its distinct *cis*-β configuration.

3.3. Chiral bisoxazoline (BOX) ligands

By employing a chiral spiro-BOX ligand in combination with a Cu(MeCN)$_4$PF$_6$ catalyst, Gouverneur and co-workers demonstrated an early example of highly enantioselective catalytic Si–H insertion between CF$_3$-containing diazo compounds and various silanes, achieving yields of up to 99% and enantioselectivities of up to 98% ee (Scheme 30).[24] The enantioenriched silane products could be stereo-retentively converted into secondary alcohols under Tamao-Fleming oxidation conditions, highlighting the synthetic utility of this chiral silane scaffold. However, the scope of this catalytic system was limited, as bulkier substrates, such as triisopropylsilane, significantly reduced the yield and enantioselectivity.

In 2018, Lin and Xie developed a cost-effective and sustainable approach to synthesize valuable chiral α-silyl esters

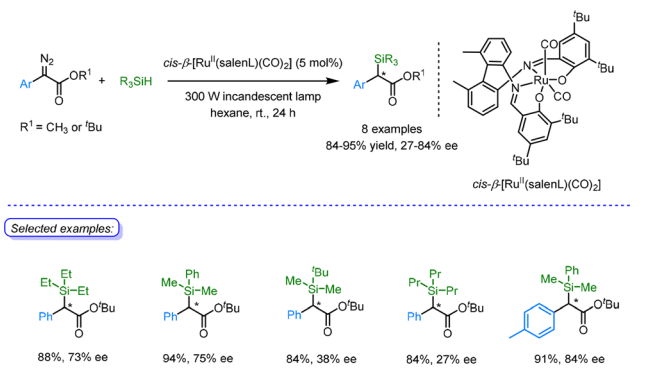

Scheme 29 Ru(II)-salen catalyzed enantioselective Si–H insertion with diazoesters.

Published on 09 June 2025. Downloaded by Shaanxi Normal University on 6/10/2025 4:15:58 AM.

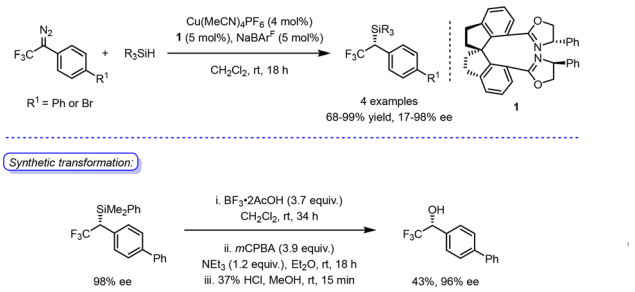

Scheme 30 Cu(I)/spiro-BOX catalyzed Si–H insertion with CF_3-containing diazo compounds and silanes.

through iron-catalyzed enantioselective Si–H bond insertion of α-diazoesters.[65] Using a chiral spiro-BOX ligand (HMSI-BOX), $Fe(OTf)_2$ as the catalyst, and $NaBAr^F$ as an additive, they evaluated a broad range of α-diazoarylacetates and silanes, achieving excellent yields (up to 99%) and high enantioselectivities (up to 96% ee). Notably, α-diazoalkylacetates showed no reactivity under these conditions (Scheme 31). Density functional theory (DFT) calculations revealed that the quintet spin state of the Fe(II)-catalyst complex was the most favorable transition state, with steric repulsion between the phenyl and ester groups dictating the enantioselectivity outcome.

Expanding beyond traditional diazo compounds as carbene precursors, Ye and Zhu explored Si–H insertion reactions involving *N*-propargyl ynamides and hydrosilanes to construct 4-silyl-substituted pyrroles under Cu(I) catalysis.[66] An asymmetric variant of this transformation was briefly investigated using a chiral BOX ligand, yielding promising results with a 52% yield and 48% ee, indicating significant potential for further optimization (Scheme 32). The proposed mechanism involves the formation of a vinyl cation intermediate, followed by hydride transfer from the silane to generate a Cu(I)-carbene species. Subsequent [1,4]-hydride shift and demetallation afford the desired product.

Most recently, Zhu and co-workers extended the catalytic Si–H bond insertion strategy to 1-borylcyclopropenes as α-boryl carbene precursors.[31] A Cu(I)/chiral BOX ligand system efficiently catalyzed the insertion reactions with hydrosilanes,

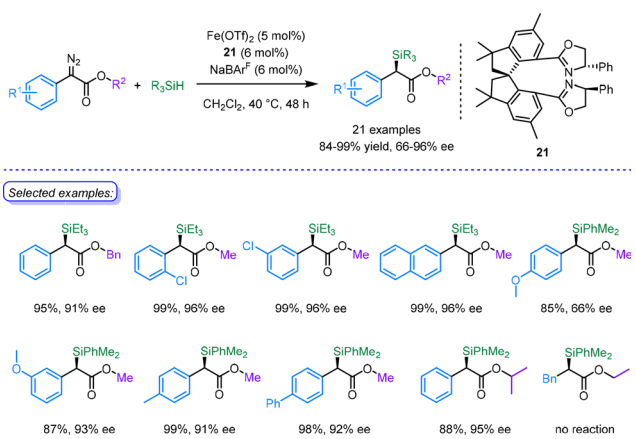

Scheme 31 Fe(II)/catalyzed Si–H insertion with chiral spiro-BOX ligand.

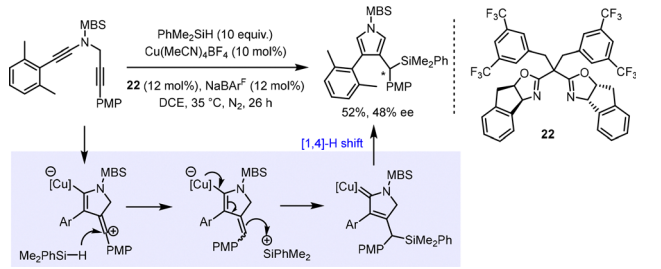

Scheme 32 Fe(II)-catalyzed Si–H insertion with chiral spiro-BOX ligand.

producing enantioenriched allylic *gem*-borylsilanes with exceptional enantioselectivities (up to 98% ee) (Scheme 33). As previously described in Scheme 6, the observed stereoselectivity originated from the specific conformation of the BPin group, allowing face shielding provided by the chiral BOX ligand to direct the nucleophilic attack preferentially from the less hindered face. The resulting chiral organosilanes demonstrated significant synthetic utility in homologation, oxidation reactions, and allylborations.

3.4. Chiral diene ligands

In addition to the well-established Rh(I)/chiral diene complex-catalyzed B–H insertion reactions, our group successfully extended this catalytic system to the challenging Si–H insertion in 2016. It is well-known that in the presence of silanes, Rh(I) complexes, represented by Wilkinson's catalyst $Rh(PPh_3)_3Cl$, initially undergo oxidative addition to the Si–H bond, triggering a hydrosilylation reaction.[67] Interestingly, when olefins are employed as ligands, the Rh(I) complex was found to catalyze the reaction through a distinct carbene insertion pathway. Using α-diazoesters and α-diazophosphonates as carbene precursors, we achieved the first Rh(I)-catalyzed enantioselective Si–H insertion. A wide range of highly enantioenriched α-silyl

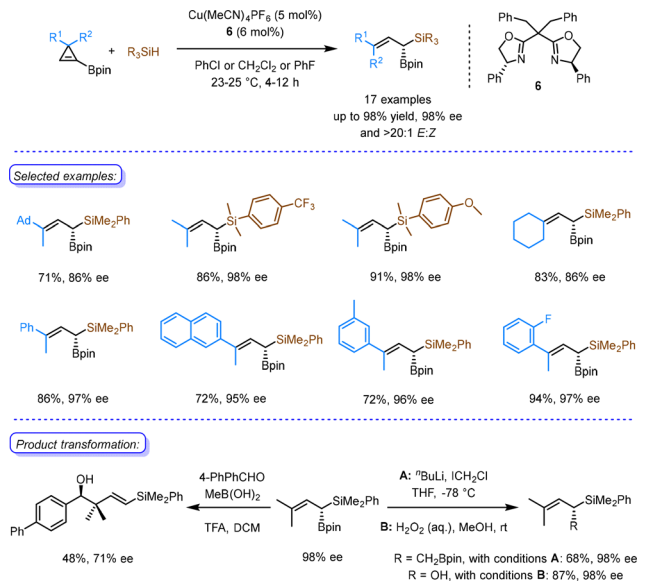

Scheme 33 Cu(I)/chiral BOX catalyzed Si–H insertion with 1-borylcyclopropenes.

This journal is © The Royal Society of Chemistry 2025

Published on 09 June 2025. Downloaded by Shaanxi Normal University on 6/10/2025 4:15:58 AM.

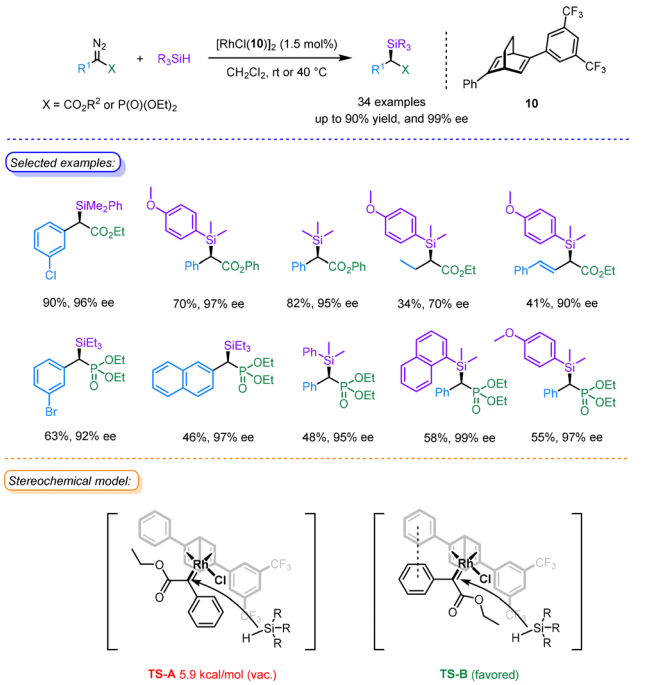

Scheme 34 Rh(I)/chiral diene catalyzed enantioselective Si–H insertion with α-diazoesters and α-diazophosphonates.

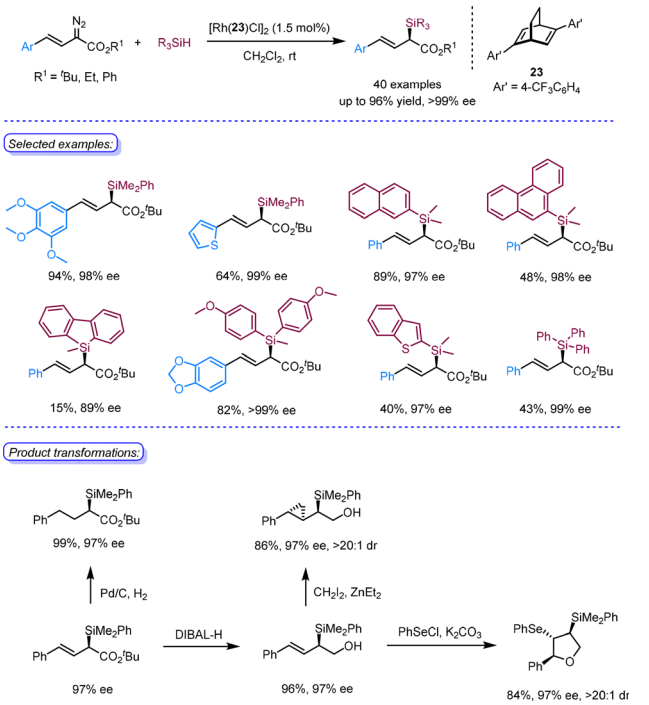

Scheme 36 Enantioselective Si–H insertion of vinyldiazoacetates catalyzed by Rh(I)/chiral diene ligand.

esters and phosphonates with enantioselectivities of up to 99% ee were accessed, facilitated by a C_1-symmetric bicyclo[2.2.2]-octadiene ligand (Scheme 34).[68] Computational studies revealed two possible transition states **A** and **B**, with transition state **B** being energetically more favorable. The Si–H bond addition preferentially occurs from the unblocked *Re*-face of transition state **B**, leading to the formation of the *R* product, which is consistent with the experimental stereochemical outcome.

Building on the above work, Perekalin expanded the application of this catalytic system to asymmetric Si–H insertion of α-aryldiazoesters with triethylsilane by employing a novel chiral diene ligand featuring tetrafluorobenzobarrelene scaffolds, as previously described for asymmetric B–H insertion (Scheme 10).[35] A range of products with 78–89% yields and enantioselectivities of up to 97% ee were obtained (Scheme 35). These results are comparable to that achieved with C_1-symmetric bicyclo[2.2.2]-octadiene ligands.

More recently, the utility of Rh(I)/chiral diene complexes in catalyzing asymmetric Si–H insertion with arylvinyldiazoacetates was further demonstrated by our group, significantly expanding the substrate scope.[69] Compared to the seminal work by Davies in 1997 using chiral dirhodium carboxylate complexes (see Scheme 21), this study demonstrated broader substrate compatibility, including heteroaryl vinyldiazoacetates and sterically demanding silanes, as well as enhanced catalytic reactivity and stereocontrol (Scheme 36). The synthetic versatility of the resulting chiral vinyl silanes was demonstrated through various transformations, such as reduction/hydrogenation, cyclization, and Simmons-Smith cyclopropanation, all of which proceeded without erosion of enantiopurity.

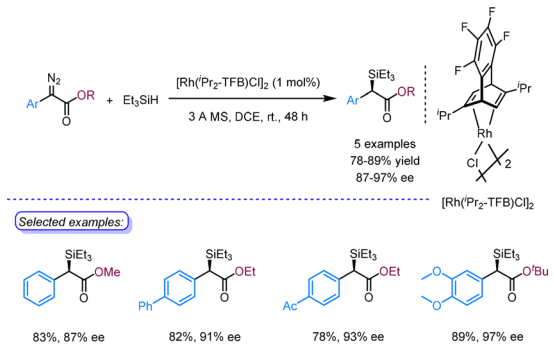

Scheme 35 Enantioselective Si–H insertion catalyzed by Rh(I)/diene ligand.

3.5. Miscellaneous

In addition to the commonly employed ligand/catalyst systems discussed above, several nature-inspired carbenoid transfer systems have been developed and evaluated for asymmetric Si–H insertion reactions. In 2012, Che and co-workers achieved a highly enantioselective Si–H insertion of aryldiazoacetates using a chiral iridium(III) complex featuring a D_4-symmetric Halterman porphyrin ligand.[70] This approach significantly broadened the scope of the reaction, delivering organosilanes with enantioselectivities of up to 91% ee and yields of up to 94% at −80 °C (Scheme 37).

Another notable asymmetric protocol, utilizing a chiral Ru(II)–Pheox catalyst as exemplified in the B–H insertion of alkyldiazoacetates (Scheme 19), was reported by Iwasa and

Published on 09 June 2025. Downloaded by Shaanxi Normal University on 6/10/2025 4:15:58 AM.

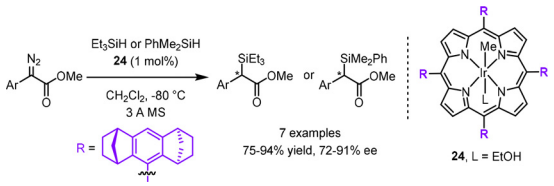

Scheme 37 Enantioselective Si–H insertion of aryldiazoacetates catalyzed by Ir(III)/porphyrin complex.

Chanthamath, enabling the simultaneous construction of both chiral carbon and silicon centers.[71] This method demonstrated broad substrate compatibility, accommodating a wide range of simple and sterically hindered α-methyldiazoesters. Notably, more sterically demanding substrates exhibited enhanced enantiocontrol and reactivity (Scheme 38). When prochiral silanes were employed, excellent enantioselectivity was maintained, although diastereoselectivity was not ideal, ranging from 58 : 42 to 79 : 21 dr. The observed enantioselectivity was primarily influenced by the steric bulk of both the diazoesters and silanes, with minimal electronic effects from the silanes.

Beyond traditional chiral ligand design, efforts have been directed toward exploring naturally occurring metalloenzymes and peptides for asymmetric transformations. Ball and co-workers developed a novel macromolecular ligand framework by ligating natural peptide sequences to the dirhodium centers of $Rh_2(TFA)_4$ through two bridging carboxylate-containing aspartate side chains, resulting in an α-helical secondary structure.[72] Using a combinatorial approach with a library of nonapeptides, the Si–H bond insertion of α-phenyldiazoacetate and $PhMe_2SiH$ was optimized, achieving an enantioselectivity of 92% ee (Scheme 39). This protocol was proved to be compatible with various diazoesters, including aryl- and vinyl-substituted diazoesters, highlighting the potential of metallopeptides in asymmetric catalysis.

In 2016, Arnold and co-workers demonstrated a groundbreaking study on the directed evolution of cytochrome *c* from

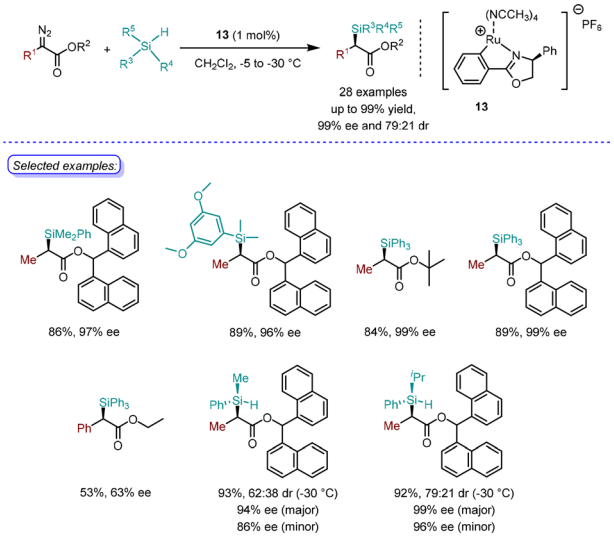

Scheme 38 Enantioselective Si–H insertion catalyzed by Ru(II)/Pheox catalyst.

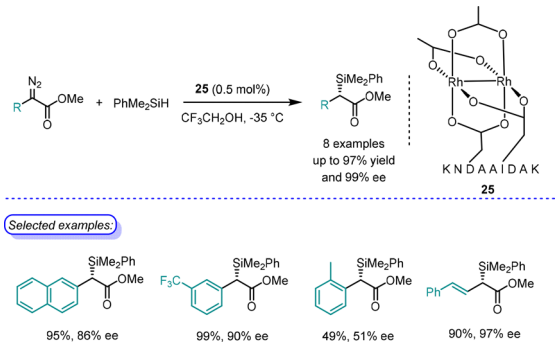

Scheme 39 Exploring the natural peptide scaffolds with dirhodium catalysts in asymmetric Si–H insertion.

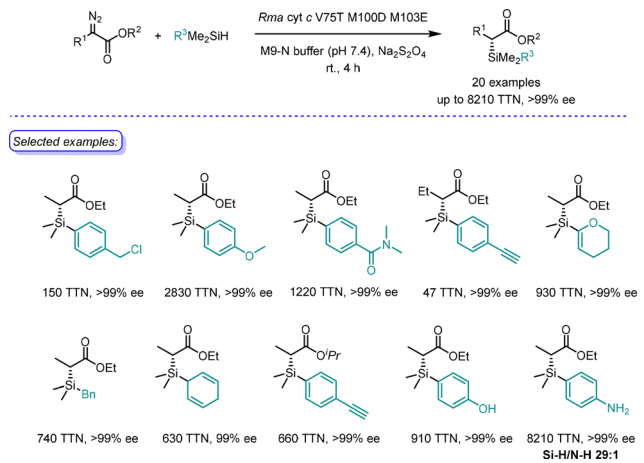

Scheme 40 Biocatalysis in asymmetric Si–H insertion.

Rma cyt *c* to catalyze enantioselective Si–C bond formation through carbene insertion, achieving enantioselectivities of >99% ee and a total turnover number (TTN) of 8210.[73] This work highlighted the remarkable ability of enzymes to perform non-natural bond-forming reactions under mild, physiological conditions (Scheme 40). The enzyme exhibited exceptional chemoselectivity, favoring Si–H insertion over N–H insertion with a product ratio of 29 : 1. Furthermore, by expressing the triple mutant in *E. coli*, the *in vivo* synthesis of organosilicon compounds was accomplished with up to 3410 TTN and 98% ee, demonstrating the feasibility of integrating silicon into biological pathways and producing Si–C bonds in living systems.

4. Ligand controlled catalytic asymmetric Ge–H insertion

While catalytic asymmetric Si–H and B–H bond insertions are well-established and widely documented, providing efficient routes to chiral organosilicon and organoboron compounds, the analogous Ge–H insertion remains underexplored. This is primarily due to several challenges, including germanium's larger covalent radius compared to carbon and silicon, its complex electronic

 This journal is © The Royal Society of Chemistry 2025

Published on 09 June 2025. Downloaded by Shaanxi Normal University on 6/10/2025 4:15:58 AM.

configuration, and the propensity of Ge–H bonds to form germanium radicals.[74] Remarkably, only two examples of catalytic Ge–H insertion have been reported to date, highlighting a significant gap in this field and underscoring the inherent challenges associated with organogermanium chemistry.

In early 2024, Zhou and co-workers addressed this gap by reporting the first chiral dirhodium spiro-phosphate-catalyzed enantioselective carbene insertion into Ge–H bonds, providing efficient access to valuable chiral organogermanium compounds.[75] This method demonstrated promising reactivity and enantioselectivity with aryl-substituted diazobenzylesters, diazo-diarylmethanes, and 1-arylpropargyl diazo derivatives (Scheme 41). DFT calculations revealed that the Ge–H insertion step is highly stereoselective, driven by the steric hindrance and electronic environment created by the dirhodium phosphate catalyst. Furthermore, the versatility of the resulting chiral organogermanes was demonstrated through their transformation into chiral alcohols, allenylgermanes, and allylgermanes.

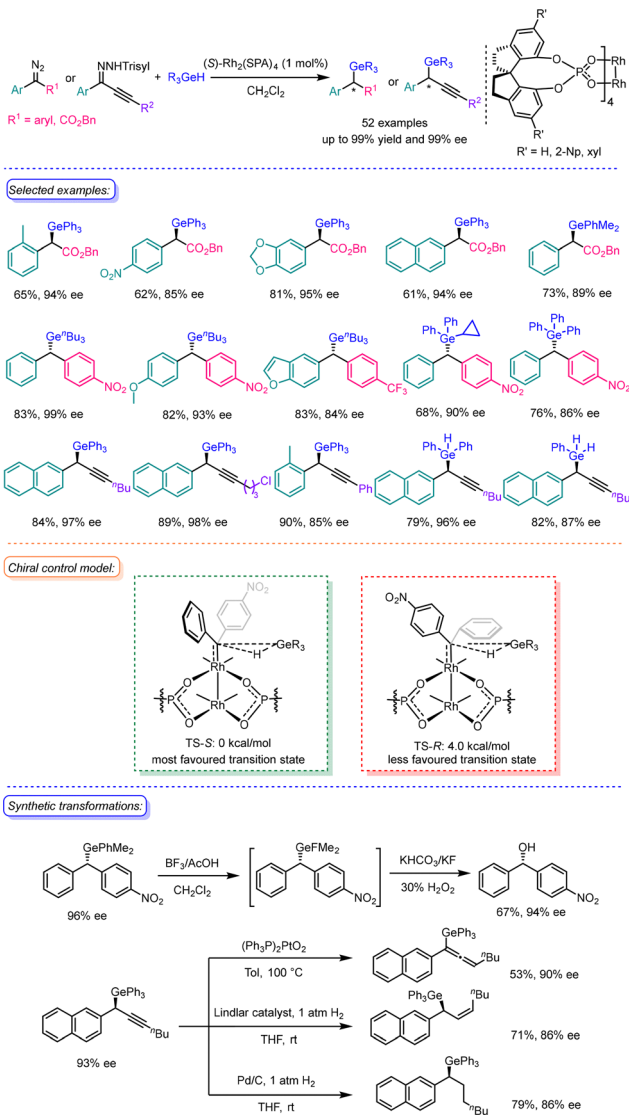

Scheme 41 Rh(II)/spiro-phosphate catalyzed Ge–H insertion.

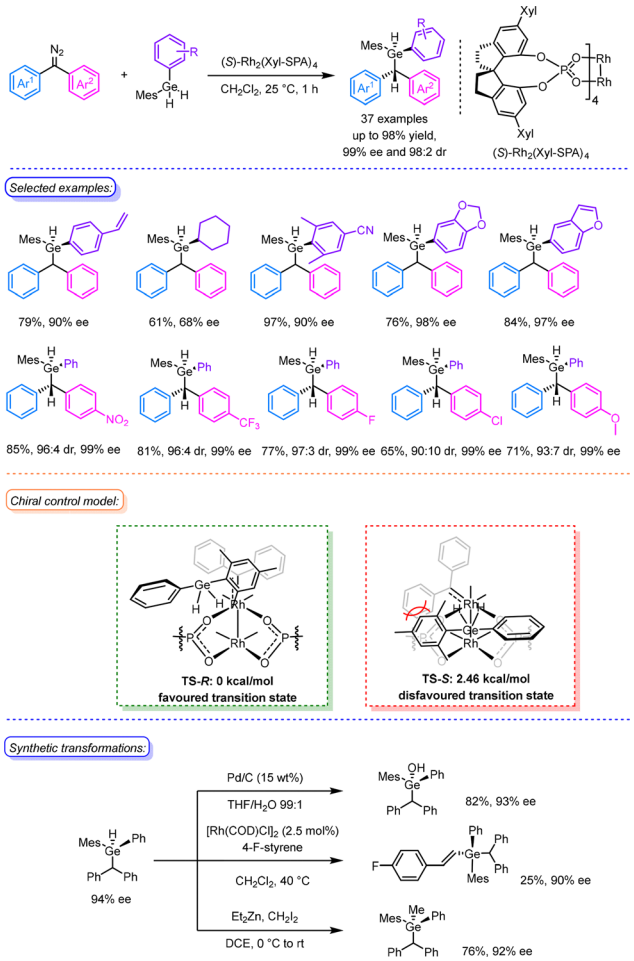

Scheme 42 Rh(II)/spiro-phosphate catalyzed desymmetric Ge–H insertion.

As a further extension of this Ge–H insertion strategy, the same group developed an elegant protocol for constructing Ge-stereogenic centers *via* chiral rhodium(II) spiro-phosphonate-catalyzed desymmetric carbene insertion into prochiral germanes.[76] This method exhibited excellent compatibility with both (hetero)aryl- and alkyl-substituted dihydrogermanes, as well as unsymmetrical diazodiarylmethanes, while maintaining high diastereo- and enantioselectivity (Scheme 42). Computational modeling indicated that the enantioselectivity arises from steric interactions between the Mes group on the dihydrogermane and the crowded chiral pocket formed by the spiro-phosphate ligands, directing the Ge–H bond to attack the rhodium carbene from the less sterically hindered side. The synthetic utility of this approach was further demonstrated through hydrogermylation, oxidation, and alkylation reactions, which effectively converted the Ge–H insertion products bearing the second Ge–H bond into enantioenriched organogermanium derivatives.

5. Conclusions

The field of catalytic asymmetric X–H insertion reactions, particularly involving metalloid–hydrogen bonds (B–H, Si–H, and Ge–H), has witnessed remarkable advancements in recent years. These

Published on 09 June 2025. Downloaded by Shaanxi Normal University on 6/10/2025 4:15:58 AM.

reactions have emerged as powerful tools for constructing diverse enantioenriched molecular scaffolds with important applications in organic synthesis, material science, and drug discovery. Key to these developments has been the strategic design of chiral ligand frameworks, such as bisoxazoline (BOX), carboxylate/phosphonate, and diene ligands, which have enabled high stereocontrol and efficiency in the synthesis of organoboranes with carbon stereogenic centers. Cu(I) and Rh(I) catalysts, in combination with BOX and diene ligands, have demonstrated exceptional enantioselectivity in accessing boron-stereogenic compounds, although challenges remain with sterically hindered substrates and certain diazo precursors. In the realm of Si–H insertion, chiral Rh(II), Rh(I), Cu(I), and Ir(III) catalytic systems have proven fundamental for constructing both carbon- and silicon-stereogenic compounds, as well as functional organosilanes. Meanwhile, the emerging field of Ge–H insertion has been pioneered by dirhodium catalysis with spiro-phosphate ligands, offering a promising route to chiral organogermanium molecules. Despite the excellent enantioselectivity and synthetic utility demonstrated in preliminary studies, the field remains underdeveloped compared to B–H and Si–H insertions, largely due to the highly reactive nature of organogermanes.

While significant progress has been made, several limitations persist, including substrate sensitivity, moderate diastereoselectivity in certain cases, and the need for extensive optimization of reaction conditions. These challenges highlight the importance of continued innovation in ligand design and catalytic systems. Looking ahead, the integration of computational modeling with experimental efforts holds great promise for overcoming these limitations by enabling the rational design of more efficient ligands and reaction pathways. Furthermore, expanding these strategies to other underexplored X–H bonds, as well as to the synthesis of boron-, silicon-, and germanium-stereogenic compounds, offers significant opportunities to enrich the methodologies available for asymmetric synthesis.

Notably, the predominance of Cu and Rh catalysts in carbene insertion reactions into metalloid–hydrogen bonds can be attributed to their well-documented efficacy in achieving high enantioselectivity and broad substrate scope, as well as their compatibility with a variety of chiral ligands. While other transition-metals such as Fe, Pd, Ag, Au, and Ir have shown success in carbene insertions into N–H, O–H and S–H bonds, their application in metalloid–hydrogen bond insertions remains less explored, demonstrating a potential area for future research.[12]

Additionally, biocatalytic approaches leveraging engineered enzymes offer an exciting and environmentally friendly alternative for highly selective X–H insertion reactions.[77] These methods not only align with the growing demand for sustainable chemistry but also open new avenues for achieving unprecedented levels of selectivity and efficiency in asymmetric catalysis. As the field continues to evolve, the synergy between transition metal catalysis, computational design, and biocatalysis is poised to drive transformative breakthroughs, ushering in a new era of innovation in asymmetric synthesis.

Data availability

No primary research results, software or code have been included, and no new data were generated or analysed as part of this review.

Conflicts of interest

There are no conflicts to declare.

Acknowledgements

We thank the National Natural Science Foundation of China (21971103), Guangdong Provincial Department of Science and Technology (2019CX01Y251), Shenzhen Key Laboratory of Small Molecule Drug Discovery and Synthesis (ZDSYS20190902093215877), and Guangdong Provincial Key Laboratory of Catalysis (2020B121201002) for financial support.

Notes and references

1 B. Marciniec, C. Pietraszuk, P. Pawluć and H. Maciejewski, *Chem. Rev.*, 2022, **122**, 3996–4090.
2 H. Yorimitsu, M. Kotora and N. T. Patil, *Chem. Rec.*, 2021, **21**, 3335–3337.
3 R. J. Grams, W. L. Santos, I. R. Scorei, A. Abad-García, C. A. Rosenblum, A. Bita, H. Cerecetto, C. Viñas and M. A. Soriano-Ursúa, *Chem. Rev.*, 2024, **124**, 2441–2511.
4 K. Yang and Q. Song, *Acc. Chem. Res.*, 2021, **54**, 2298–2312.
5 Y. Wu and P. Wang, *Angew. Chem., Int. Ed.*, 2022, **61**, e202205382.
6 J.-H. Ye, L. Quach, T. Paulisch and F. Glorius, *J. Am. Chem. Soc.*, 2019, **141**, 16227–16231.
7 M. Yi, X. Wu, L. Yang, Y. Yuan, Y. Lu and Z. Zhang, *J. Org. Chem.*, 2024, **89**, 12583–12590.
8 X. Zhao, G. Wang and A. S. K. Hashmi, *ChemCatChem*, 2021, **13**, 4299–4312.
9 L. Li, W.-S. Huang, Z. Xu and L.-W. Xu, *Sci. China: Chem.*, 2023, **66**, 1654–1687.
10 M.-Y. Huang and S.-F. Zhu, *Chem. Catal.*, 2022, **2**, 3112–3139.
11 V. Carreras, N. Tanbouza and T. Ollevier, *Synthesis*, 2020, 79–94.
12 B. D. Bergstrom, L. A. Nickerson, J. T. Shaw and L. W. Souza, *Angew. Chem., Int. Ed.*, 2021, **60**, 6864–6878.
13 M.-Y. Huang and S.-F. Zhu, *Chem. Sci.*, 2021, **12**, 15790–15801.
14 M. Braun, *Eur. J. Org. Chem.*, 2024, e202400052.
15 Y. Guo, B. Zu, C. Du Chen and C. He, *Chin. J. Chem.*, 2024, **42**, 2401–2411.
16 X. Li, G. Zhang and Q. Song, *Chem. Commun.*, 2023, **59**, 3812–3820.
17 A. Abdou-Mohamed, C. Aupic, C. Fournet, J.-L. Parrain, G. Chouraqui and O. Chuzel, *Chem. Soc. Rev.*, 2023, **52**, 4381–4391.

 This journal is © The Royal Society of Chemistry 2025

Published on 09 June 2025. Downloaded by Shaanxi Normal University on 6/10/2025 4:15:58 AM.

18 D. Chen, X. Zhang, W.-Y. Qi, B. Xu and M.-H. Xu, *J. Am. Chem. Soc.*, 2015, **137**, 5268–5271.
19 J.-M. Yang, Z.-Q. Li, M.-L. Li, Q. He, S.-F. Zhu and Q.-L. Zhou, *J. Am. Chem. Soc.*, 2017, **139**, 3784–3789.
20 R. Connon, B. Roche, B. V. Rokade and P. J. Guiry, *Chem. Rev.*, 2021, **121**, 6373–6521.
21 Q.-Q. Cheng, S.-F. Zhu, Y.-Z. Zhang, X.-L. Xie and Q.-L. Zhou, *J. Am. Chem. Soc.*, 2013, **135**, 14094–14097.
22 X. Li and D. P. Curran, *J. Am. Chem. Soc.*, 2013, **135**, 12076–12081.
23 Q.-Q. Cheng, S.-F. Zhu, H. Xu and Q.-L. Zhou, *Acta Chim. Sin.*, 2015, **73**, 326–329.
24 S. Hyde, J. Veliks, B. Liégault, D. Grassi, M. Taillefer and V. Gouverneur, *Angew. Chem., Int. Ed.*, 2016, **55**, 3785–3789.
25 L. Li, K. Yu, H. An, X. Cai and Q. Song, *Chem. Sci.*, 2024, **15**, 7130–7135.
26 T.-Y. Wang, X.-X. Chen, D.-X. Zhu, L. W. Chung and M.-H. Xu, *Angew. Chem., Int. Ed.*, 2022, **61**, e202207008.
27 J. Barluenga, L. Riesgo, L. A. López, E. Rubio and M. Tomás, *Angew. Chem., Int. Ed.*, 2009, **48**, 7569–7572.
28 D. Drikermann, R. S. Mößel, W. K. Al-Jammal and I. Vilotijevic, *Org. Lett.*, 2020, **22**, 1091–1095.
29 M.-Y. Huang, Y.-T. Zhao, H. Chai, C.-D. Zhang and S.-F. Zhu, *CCS Chem.*, 2022, **4**, 1232–1237.
30 M.-Y. Huang, Y.-T. Zhao, C.-D. Zhang and S.-F. Zhu, *Angew. Chem., Int. Ed.*, 2022, **61**, e202203343.
31 M.-Y. Huang, J.-B. Zhao, C.-D. Zhang, Y.-J. Zhou, Z.-S. Lu and S.-F. Zhu, *J. Am. Chem. Soc.*, 2024, **146**, 9871–9879.
32 G. Zhang, Z. Zhang, M. Hou, X. Cai, K. Yang, P. Yu and Q. Song, *Nat. Commun.*, 2022, **13**, 2624.
33 G. Zhang, X. Cai, J. Jia, B. Feng, K. Yang and Q. Song, *ACS Catal.*, 2023, **13**, 9502–9508.
34 Y. Huang and T. Hayashi, *Chem. Rev.*, 2022, **122**, 14346–14404.
35 N. M. Ankudinov, D. A. Chusov, Y. V. Nelyubina and D. S. Perekalin, *Angew. Chem., Int. Ed.*, 2021, **60**, 18712–18720.
36 N. M. Ankudinov, A. A. Komarova, E. S. Podyacheva, D. A. Chusov, A. A. Danshina and D. S. Perekalin, *Chem. Commun.*, 2024, **60**, 8601–8604.
37 W. Xu, T. Yamakawa, M. Huang, P. Tian, Z. Jiang and M.-H. Xu, *Angew. Chem., Int. Ed.*, 2024, **63**, e202412193.
38 J.-G. Liu, B. Liu, Z. Li and M.-H. Xu, *CCS Chem.*, 2024, 1–12.
39 J. Hansen and H. M. L. Davies, *Coord. Chem. Rev.*, 2008, **252**, 545–555.
40 F. G. Adly and A. Ghanem, *Chirality*, 2014, **26**, 692–711.
41 Y. Pang, Q. He, Z.-Q. Li, J.-M. Yang, J.-H. Yu, S.-F. Zhu and Q.-L. Zhou, *J. Am. Chem. Soc.*, 2018, **140**, 10663–10668.
42 Y.-T. Zhao, Y.-X. Su, X.-Y. Li, L.-L. Yang, M.-Y. Huang and S.-F. Zhu, *Angew. Chem., Int. Ed.*, 2021, **60**, 24214–24219.
43 H.-N. Zou, Y.-T. Zhao, L.-L. Yang, M.-Y. Huang, J.-W. Zhang, M.-L. Huang and S.-F. Zhu, *ACS Catal.*, 2022, **12**, 10654–10660.
44 H.-N. Zou, M.-L. Huang, M.-Y. Huang, Y.-X. Su, J.-W. Zhang, X.-Y. Zhang and S.-F. Zhu, *Chem. Sci.*, 2023, **14**, 9186–9190.
45 N. Otog, S. Chanthamath, I. Fujisawa and S. Iwasa, *Eur. J. Org. Chem.*, 2021, 1564–1567.
46 S. B. J. Kan, X. Huang, Y. Gumulya, K. Chen and F. H. Arnold, *Nature*, 2017, **552**, 132–136.
47 X. Huang, M. Garcia-Borràs, K. Miao, S. B. J. Kan, A. Zutshi, K. N. Houk and F. H. Arnold, *ACS Cent. Sci.*, 2019, **5**, 270–276.
48 K. Chen, X. Huang, S.-Q. Zhang, A. Z. Zhou, S. B. J. Kan, X. Hong and F. H. Arnold, *Synlett*, 2019, 378–382.
49 L.-J. Sun, H. Wang, J.-K. Xu, W. Niu, S.-Q. Gao and Y.-W. Lin, *Org. Lett.*, 2024, **26**, 8872–8877.
50 J.-L. Panayides, D. L. Riley, F. Hasenmaile and W. A. L. van Otterlo, *RSC Med. Chem.*, 2024, **15**, 3286–3344.
51 J. R. Henstock, L. T. Canham and S. I. Anderson, *Acta Biomater.*, 2015, **11**, 17–26.
52 R. T. Buck, M. P. Doyle, M. J. Drysdale, L. Ferris, D. C. Forbes, D. Haigh, C. J. Moody, N. D. Pearson and Q.-L. Zhou, *Tetrahedron Lett.*, 1996, **37**, 7631–7634.
53 H. M. L. Davies, T. Hansen, J. Rutberg and P. R. Bruzinski, *Tetrahedron Lett.*, 1997, **38**, 1741–1744.
54 M. Ge and E. J. Corey, *Tetrahedron Lett.*, 2006, **47**, 2319–2321.
55 M.-Y. Huang, J.-M. Yang, Y.-T. Zhao and S.-F. Zhu, *ACS Catal.*, 2019, **9**, 5353–5357.
56 J. R. Jagannathan, J. C. Fettinger, J. T. Shaw and A. K. Franz, *J. Am. Chem. Soc.*, 2020, **142**, 11674–11679.
57 L.-L. Yang, D. Evans, B. Xu, W.-T. Li, M.-L. Li, S.-F. Zhu, K. N. Houk and Q.-L. Zhou, *J. Am. Chem. Soc.*, 2020, **142**, 12394–12399.
58 L.-L. Yang, J. Ouyang, H.-N. Zou, S.-F. Zhu and Q.-L. Zhou, *J. Am. Chem. Soc.*, 2021, **143**, 6401–6406.
59 J. F. Larrow, E. N. Jacobsen, Y. Gao, Y. Hong, X. Nie and C. M. Zepp, *J. Org. Chem.*, 1994, **59**, 1939–1942.
60 Y.-Z. Zhang, S.-F. Zhu, L.-X. Wang and Q.-L. Zhou, *Angew. Chem., Int. Ed.*, 2008, **47**, 8496–8498.
61 J. Wu, Y. Chen and J. S. Panek, *Org. Lett.*, 2010, **12**, 2112–2115.
62 V. Carreras, C. Besnard, V. Gandon and T. Ollevier, *Org. Lett.*, 2019, **21**, 9094–9098.
63 Y. Yasutomi, H. Suematsu and T. Katsuki, *J. Am. Chem. Soc.*, 2010, **132**, 4510–4511.
64 C. L. Lee, D. Chen, X.-Y. Chang, Z. Tang and C.-M. Che, *Organometallics*, 2020, **39**, 2642–2652.
65 H. Gu, Z. Han, H. Xie and X. Lin, *Org. Lett.*, 2018, **20**, 6544–6549.
66 E.-H. Huang, Y.-Q. Zhang, D.-Q. Cui, X.-Q. Zhu, X. Li and L.-W. Ye, *Org. Lett.*, 2022, **24**, 196–201.
67 S. M. Jackson, D. M. Chisholm, J. S. McIndoe and L. Rosenberg, *Eur. J. Inorg. Chem.*, 2011, 327–330.
68 D. Chen, D.-X. Zhu and M.-H. Xu, *J. Am. Chem. Soc.*, 2016, **138**, 1498–1501.
69 Z. Li, J.-G. Liu, W.-P. Zhang and M.-H. Xu, *Adv. Synth. Catal.*, 2024, **366**, 2514–2518.
70 J.-C. Wang, Z.-J. Xu, Z. Guo, Q.-H. Deng, C.-Y. Zhou, X.-L. Wan and C.-M. Che, *Chem. Commun.*, 2012, **48**, 4299–4301.
71 Y. Nakagawa, S. Chanthamath, I. Fujisawa, K. Shibatomi and S. Iwasa, *Chem. Commun.*, 2017, **53**, 3753–3756.
72 R. Sambasivan and Z. T. Ball, *J. Am. Chem. Soc.*, 2010, **132**, 9289–9291.
73 S. B. J. Kan, R. D. Lewis, K. Chen and F. H. Arnold, *Science*, 2016, **354**, 1048–1051.

74 W. Lin, L.-Q. Ren, C. D. Chen, X. Han, L. Zhang, Z. Chen, J. Guo and C. He, *CCS Chem.*, 2024, **0**, 1–11.
75 A.-C. Han, X.-G. Zhang, L.-L. Yang, J.-B. Pan, H.-N. Zou, M.-L. Li, L.-J. Xiao and Q.-L. Zhou, *Chem. Catal.*, 2024, **4**, 100826.
76 A.-C. Han, L.-J. Xiao and Q.-L. Zhou, *J. Am. Chem. Soc.*, 2024, **146**, 5643–5649.
77 Y. Yang and F. H. Arnold, *Acc. Chem. Res.*, 2021, **54**, 1209–1225.

Published on 09 June 2025. Downloaded by Shaanxi Normal University on 6/10/2025 4:15:58 AM.

 This journal is © The Royal Society of Chemistry 2025